

# Degeneracy and metallic character in free and confined weakly coupled plasmas: with and without electric field

Neetik Mukherjee\* and Amlan K. Roy†

*Department of Chemical Sciences, IISER Kolkata,*

*Mohanpur-741246, Nadia, WB, India*

## Abstract

Incidental degeneracy and metallic character is probed for weakly coupled plasmas in free and confined environments. The generality of incidental degeneracy in quantum mechanical systems is discussed and demonstrated. It is a fundamental property of free and confined quantum systems. In plasmas, at a given  $n, \ell$  state there exists  $\frac{(n-\ell)(n-\ell+1)}{2}$  number of incidental degenerate states. Such degeneracy condition involves shell confinement model, where a particle is encaged inside two concentric sphere. Apart from that, Dipole oscillator strength and polarizability are examined in free and confined conditions for ground and some low-lying  $\ell$  states. In excited states, negative  $\alpha^{(1)}$  is recorded. Further, metallic behavior of H-like plasmas is investigated. The impact of external static electric field on these degeneracy, dipole OS, dipole polarizability are examined with utmost interest. Pilot calculation are done with, (i) Debye plasmas and, (ii) Exponential screened coulomb potentials employing the Generalized pseudo-spectral (GPS) method.

**Keywords:** Shell confinement, incidental degeneracy, polarizabilities, metallic character

---

\*Electronic address: pchem.neetik@gmail.com.

†Corresponding author. Email: akroy@iiserkol.ac.in, akroy6k@gmail.com.

## I. INTRODUCTION

Hydrogen atom represents the simplest two-body system consisting of a proton and an electron. The Schrödinger equation (SE) offers exact analytical closed-form solution in both non-relativistic and relativistic domain. Probing hydrogenic systems is extremely important, as they can act as a precursor to understand the quantum effects in more complex structure [1, 2]. In the visible universe, hydrogen constitutes more than 90% of all atoms and contributes three quarter of its mass [2]. Further, it is a well known fact that, in the inner core of the Sun, hydrogen fuses together to form helium and release energy. This is the source of energy in our solar system. Further, its abundance in the interiors of Jupiter and Saturn is well known. In these planets, it is present in both metallic and liquid form, which is responsible for their origin of magnetosphere [3–6]. To be precise, most of the celestial bodies ranging from giant planets to recently discovered brown dwarfs [7] are primarily composed of dense hydrogen and helium plasmas. In recent years the investigation of atomic processes in plasma environment has become a subject of topical interest. It elicits the screening effect of plasma on atoms embedded in such situations.

High energy-density physics covers a broad range of plasmas from very hot to dense conditions. In this scenario, there occurs a coupling between plasma electrons and immersed atoms, leading to a change in electronic properties. The composite influences of plasma free-electron density ( $n_e$ ) and temperature ( $T$ ) plays a crucial role in stabilizing a bound state by controlling the strength of this coupling. The coupling parameter ( $\Gamma$ ) is defined as [8–10],

$$\Gamma = \frac{r_-}{a} = \frac{E_{\text{coulomb}}}{E_{\text{thermal}}} = \frac{Q^2}{aT}, \quad (1)$$

where  $r_-$  is the critical radius of a circular volume beyond which no plasma electron can approach the atom [8],  $a = \left(\frac{3}{4\pi n_e}\right)^{\frac{1}{3}}$  is the inter-particle spacing, called *ion-sphere radius*,  $Q$  denotes the charge of ion.  $\Gamma \ll 1$  signifies high  $T$ , low  $n_e$  condition (weakly coupled), while,  $\Gamma \gg 1$  represents low  $T$ , high  $n_e$  situation (strongly coupled). In a given plasma, the correlated many-particle interactions are described by an average screening potential, incorporating the collective effects due to the presence of charged cloud [11].

In a dense plasma, the competing effect of  $n_e$  and  $T$  are modulated through Debye length,  $\lambda_D = \left(\frac{T}{4\pi Q^2 n_e}\right)^{\frac{1}{2}}$ . At high  $T$  and low  $n_e$ ,  $\lambda_D$  possesses higher value, and as a consequence, offers greater number of bound states. On the contrary,  $\lambda_D$  decreases at low  $T$  and high  $n_e$ , leading to a decrease in the count of bound states. Further, the plasma-tail effect (emerges

due to the existence of asymptotic part in potential) appears in the picture with rise in  $T$ . The simplest plasma condition is introduced by invoking a prototypical Debye-Hückel potential (DP), with the form:  $V_1(r) = -\frac{Z}{r}e^{-\frac{r}{\lambda_D}}$  ( $Z$  is nuclear charge). In last two decades, DP was investigated vigorously with utmost attention. The effect of plasma screening on the energy spectrum [1, 12–14], virial and Hellmann-Feynman theorems [15], two proton transitions [2, 16], transition probabilities connecting electron-impact excitation [17–19], inelastic electron-ion scattering [20, 21], Fisher information, Shannon entropy, statistical complexities [22] etc., have been studied. Numerical values of critical screening constant ( $\lambda^{(c)}$ ) for ground and low-lying excited states were presented in [23]. Recently, an empirical relation between  $\lambda_{n,\ell}^{(c)}$  and  $Z$  was proposed in [10]. The dynamic plasma screening on DP was investigated in [24–27]. The relativistic correction on plasma screening was also considered [28]. Influence of external static electric field on energy spectrum of DP is also studied [13]. Spectroscopic properties together with multipole oscillator strength (OS) and static multipole polarizabilities were evaluated for H-like atoms under the influence of DP [29–33] using various numerical methods. A time-dependent variation perturbation approach was adopted to calculate transition probability, OS, static dipole polarizability for ground state at varied  $\lambda_D$  values [34]. Recently, a generalized pseudo spectral (GPS) method is employed to give high-quality results of OS and polarizabilities in ground and excited states [35]. Several well known methods like, integration based shooting technique [36], linear variation method [37], numerical symplectic integration method [30–32], mean excitation energy based approximation formula [33], etc., were also invoked to extract these properties. The hyperpolarizability of H atom under spherically confined DP was estimated in [38]. Further, polarizabilities are also computed for confined DP plus ring-shaped potentials [39]. In the above references, however, calculations were mostly limited to ground state. In a recent work, multipole ( $k = 1 - 4$ ) OS, and subsequent polarizabilities are reported for  $1s, 2s$  states of *confined* DP [10].

The exponential cosine screened Coulomb potential (ECSCP), is expressed as,  $V_2(r) = -\frac{Z}{r}e^{-\frac{r}{\lambda_D}} \cos(\frac{r}{\lambda_D})$ , exerts a stronger effect compared to DP. The existence of oscillatory part manifests in a combined screening and wake effect around a slow-moving test charge in high  $n_e$ , low  $T$  plasma. The cosine term drives the quantum force enacting on plasma electrons to predominate over statistical pressure exerted by plasmas [40, 41]. In quantum plasma,  $\lambda_D$  depends on the wave number of electron. Its eigenvalue and eigenfunctions

were studied in a number of methods, *viz.*, perturbation and variation [42], Padé scheme [43], shooting [44], SUSY perturbation [45], asymptotic iteration [46], Laguerre polynomial [47], variation using hydrogenic wave functions [48], J-matrix [49], GPS [50], basis expansion method with Slater-type orbitals [51], symplectic integration [52], etc. The influence of  $\lambda_D$  on energy spectrum [13, 14], photoionization cross-section [47, 53], electron-impact excitation [19], etc., has been probed as well. Similar to DP, attempt was made to determine the characteristic  $\lambda_D$  beyond which, the bound state ceases to exist [10, 54]. The laser-induced excitation on confined H atom (CHA) in ECSCP was reported in terms of laser pulse,  $r_c, \lambda_D$  using Bernstein-polynomial [55]. Variations of  $f^{(1)}, \alpha^{(1)}$  against  $\lambda_D$  were reported in [41, 44, 45, 51, 52, 56]. But, like DP, ECSCP in *confined environment* has not been investigated so far in a sufficiently thorough fashion. Only some limited recent works on  $f^{(k)}, \alpha^{(k)}$  ( $k = 1 - 4$ ) for  $1s, 2s$  states [10] and  $\alpha^{(1)}$  for confined ECSCP in a ring-shaped potential [39] are available.

The concept of confinement introduces several astonishing change in chemical and physical properties in a given quantum system. This happens due to the rearrangement of atomic orbitals in such scenario [57, 58]. In this endeavour, it is pertinent to discuss behavior of hydrogen under stressed condition. Because under such situation (which can arise due to external high pressure) it can exhibit metallic character [6, 59–61], which triggers superconductivity and superfluidity at certain optimum  $T$  and  $P$  [62, 63]. Actually, several decades ago, in 1935, it was proposed that molecular hydrogen would become an atomic metal at certain a characteristic high pressure [64]. In the new millennium, discovery and development of modern experimental techniques have made it possible to investigate these phenomena [59, 61]. Raman and visible transition spectroscopy reveals that, at high pressure (200Gpa – 315Gpa), several phase transitions occur leading to new state of hydrogen having metallic character [3, 59, 65]. With an increase in external pressure, conductivity increases and resistivity decreases [66]. Moreover, in 1968, it was proposed that, metallic modification of hydrogen will guide us to high-temperature superconductor [67]. In a recent work, this feature was observed experimentally in room temperature under 325 Gpa [68]. In theoretical perspective, metallic behavior of H-atom in ground state was in reported in [69] by employing the *Herzfeld criterion* for insulator  $\rightarrow$  metal conversion [70]. Lately, further exploration has revealed that, in H atom, this occurs only in case of  $\ell = 0$  orbitals [71]. In chemistry, the shell confinement condition can be illustrated by citing the examples of

trapping of an atom/molecule within *metal organic framework* [72, 73], inside fullerene cage and zeolite cavity [74]. The sintering effect gets minimised; as a consequence the catalytic activity and thermal stability of certain *noble* metals get improved [73, 75–78]. Further, such condition amplifies photoluminescence character in nano crystals by reducing non-radiative Auger processes [72, 79] and dispels defects in polymer crystals [80, 81] etc. Shell confinement plays key role in energy storage [82–84] and therapeutics [85] and pollution control [86, 87]. After having such multipurpose applications, shell confinement model has rarely been studied. Hence the literature is very scarce.

We know that, *incidental degeneracy* is achieved when the energy of confined state equals that of an unconfined state. For this to happen, the impenetrable boundary should be placed at the position of *radial nodes* of unconfined state [71, 88]. Such degeneracy introduces a *shell-confined* model, where a H atom was confined within two concentric spheres of inner ( $R_a$ ) outer ( $R_b$ ) radii. In this context, our primary objective is to pursue *incidental degeneracy and metallic character* in two prototypical plasmas, namely (i) DP and ii) EC-SCP. Towards this goal, we consider  $f^{(k)}$  and  $\alpha^{(k)}$  ( $k = 1$ ) in ground and excited states. The dependency of incidental degeneracy upon principal ( $n$ ) and orbital ( $\ell$ ) quantum numbers is critically explored. It directs us to evaluate the correct number of such degenerate states related with a given plasma energy in free condition. Moreover, we also examine the impact of external electric field on this degeneracy and metallic behavior (via  $\alpha^{(1)}$ ) in hydrogenic plasma. Pilot calculations are done by invoking the GPS method. To the best of our knowledge, most of the results are reported here for first time. The article is constructed in following parts: Sec. II illustrate a brief description about the formalism used in present work. We discuss about the origin of incidental degeneracy in Section III. Section IV portrays a thorough discussion of results. Finally, we conclude with a few remarks in Sec. V.

## II. THEORETICAL FORMALISM

The radial Schrödinger equation (SE) for a single particle spherically confined system is given (atomic unit employed unless otherwise stated) as,

$$\left[ -\frac{1}{2} \frac{d^2}{dr^2} + \frac{\ell(\ell+1)}{2r^2} + V_e(r) + V_c(r) \right] \psi_{n,\ell}(r) = \mathcal{E}_{n,\ell} \psi_{n,\ell}(r), \quad (2)$$

Whereas,  $V_e = Fr \cos \theta$  illustrates the *external electric field*. In field free cases,  $F = 0$  or  $\theta = \frac{\pi}{2}$ . In present case, calculations are done considering  $\theta$  as parameter. Therefore, the Overall SE in spherical polar coordinate can be separable into radial and angular part.

Further,  $V_c$  is the desired confined potential given below [69, 88],

$$V_c(r) = \begin{cases} = v(r) & \text{for } R_a \leq r \leq R_b \\ = \infty & \text{for } 0 \leq r \leq R_a \\ = \infty & \text{for } r \geq R_b. \end{cases} \quad (3)$$

$v(r)$  is the generalised plasma potential, which is expressed in the following form,

$$v(r) = -\frac{Z}{r}(1 + br)e\left(-\frac{r}{\lambda}\right) \cos\left(c \frac{r}{\lambda}\right), \quad (4)$$

where  $b, c$  are real numbers.

1.  $b = 0, c = 0$ , represents DP with the form,

$$v(r) = -\frac{Z}{r}e\left(-\frac{r}{\lambda_1}\right). \quad (5)$$

2.  $b = 0, c \neq 0$ , demonstrates ECSCP, which is expressed as,

$$v(r) = -\frac{Z}{r}e\left(-\frac{r}{\lambda_2}\right) \cos\left(c \frac{r}{\lambda_2}\right). \quad (6)$$

For calculation purpose  $c = 1$ .

Here,  $Z$  is the nuclear charge. Here,  $V_c(r)$  will be referred as generalised confined condition (GCS). Depending upon the values of  $R_a, R_b$ , four distinct conditions can be envisaged, they are,

1. When  $R_a = 0, R_b = \infty \rightarrow$  *free condition* (FC).
2. When  $R_a = 0, R_b = r_c$ , a finite number  $\rightarrow$  *confined situation* (CS).
3. When  $R_a \neq 0, R_b \neq \infty$ , with  $R_a, R_b$  finite,  $\rightarrow$  *shell confined condition* (SCC).
4. If  $R_a \neq 0, R_b = \infty, \rightarrow$  *left confined situation* (LCS).

In order to estimate the energy, spectroscopic properties the GPS method was invoked. Over the time, it has been successfully used to calculate several bound-state properties of various central potentials [89–96].

### A. Multipole polarizability

The static multipole polarizability can be conveniently written as,

$$\alpha_i^{(k)} = \alpha_i^{(k)}(\text{bound}) + \alpha_i^k(\text{continuum}). \quad (7)$$

Conventionally  $\alpha_i^{(k)}$  is expressed in sum-over states form [36]. However it can also be directly estimated by adopting the standard perturbation theory[97]. Eq. (8) modifies to,

$$\begin{aligned} \alpha_i^{(k)} &= \sum_n \frac{f_{ni}^{(k)}}{(\mathcal{E}_n - \mathcal{E}_i)^2} - c \int \frac{|\langle R_i | r^k Y_{kq}(\mathbf{r}) | R_{ep} \rangle|^2}{(\mathcal{E}_{ep} - \mathcal{E}_i)} d\epsilon, \\ \alpha_i^{(k)}(\text{bound}) &= \sum_n \frac{f_{ni}^{(k)}}{(\Delta\mathcal{E}_{ni})^2}, \quad \alpha_i^k(\text{continuum}) = c \int \frac{|\langle R_i | r^k Y_{kq}(\mathbf{r}) | R_{ep} \rangle|^2}{(\mathcal{E}_{ep} - \mathcal{E}_i)} d\epsilon. \end{aligned} \quad (8)$$

In Eq. (8), the first and second terms indicate bound and continuum contributions respectively,  $f_{ni}^{(k)}$  is the multipole oscillator strength ( $k$  is a positive integer),  $c$  is a *real* constant depends only on  $\ell$  quantum number. Here,  $f_{ni}^{(k)}$  is normally expressed as,

$$f_{ni}^{(k)} = \frac{8\pi}{(2k+1)} \Delta\mathcal{E}_{ni} |\langle r^k Y_{kq}(\mathbf{r}) \rangle|^2. \quad (9)$$

Illustrating the initial ( $|n\ell m\rangle|n\ell m\rangle$ ) and final ( $|n'\ell' m'\rangle$ ) states one can easily derive,

$$f_{ni}^{(k)} = \frac{8\pi}{(2k+1)} \Delta\mathcal{E}_{ni} \frac{1}{2\ell+1} \sum_m \sum_{m'} |\langle n'\ell' m' | r^k Y_{kq}(\mathbf{r}) | n\ell m \rangle|^2. \quad (10)$$

Wigner-Eckart theorem and sum rule for  $3j$  symbol further leads to,

$$f_{ni}^{(k)} = 2 \frac{(2\ell'+1)}{(2k+1)} \Delta\mathcal{E}_{ni} |\langle r^k \rangle_{n\ell}^{n'\ell'}|^2 \left\{ \begin{matrix} \ell' & k & \ell \\ 0 & 0 & 0 \end{matrix} \right\}^2. \quad (11)$$

The transition matrix element is given by following radial integral,

$$\langle r^k \rangle = \int_0^\infty R_{n'\ell'}(r) r^k R_{n\ell}(r) r^2 dr. \quad (12)$$

Note that,  $f_{ni}^{(k)}$  depends only on  $n, \ell$ . We compute  $f^{(1)}$ ,  $\alpha^{(1)}$ , for states with  $\ell = 0 - 2$ . It is necessary to point out the multipole oscillator strength sum rule as,

$$S^{(k)} = \sum_m f^{(k)} = k \langle \psi_i | r^{(2k-2)} | \psi_i \rangle, \quad (13)$$

where the summation incorporates all the bound and continuum states.

### 1. Herzfeld criteria for Metallic Character

According to Herzfeld criteria [70], insulator to metallic conversion occurs after attaining a threshold volume having the form,

$$V = \frac{4}{3}\pi\alpha_d, \quad (14)$$

where  $\alpha_d$  is the dipole polarizability of the atom or molecule. Let us assume that, an atom or a molecule is trapped inside a concentric sphere of radius  $r_c$ , then, Eq. (14) modifies to the form,

$$V = \frac{4}{3}\pi r_c^3 = \frac{4}{3}\pi\alpha_d \quad (15)$$

$$r_c^3 = \alpha_d.$$

Further, considering that, the particle is confined inside a spherical shell having inner and outer radius  $R_a$  and  $R_b$  respectively. Therefore, Eq. (14) becomes,

$$V = \frac{4}{3}\pi (R_b^3 - R_a^3) = \frac{4}{3}\pi\alpha_d \quad (16)$$

$$(R_b^3 - R_a^3) = \alpha_d.$$

It is important to point out that, at  $R_a = 0$  Eq. (16) reduces to Eq. (15), therefore  $R_b = r_c$ . However, in H-like atoms it has been found that, for a arbitrary  $n, \ell$  state  $\alpha_d$  decreases with reduction in  $r_c$  [10]. As a matter of fact  $V > \alpha_d$ , hence metallic character is not seen. On the contrary,  $\alpha_d$  increases with decrease in  $\Delta R = (R_b - R_a)$ . In a given  $(n, 0)$  state, for each of these  $R_b$  values there exist a characteristics  $R_a$  values after which  $\alpha_d > (R_b^3 - R_a^3)$ , as a results metallic character is seen [71]. In the present endeavour, we aim to verify this idea for plasma systems.

### III. ORIGIN OF INCIDENTAL DEGENERACY

In quantum mechanics a *free particle* of mass  $a$  is allowed to move in all direction in space with energy  $k^2/2a$  ( $k$  is a real number). Therefore, a free particle possesses any +ve value of energy. The introduction of the boundary condition  $\psi_n(x) = 0$  at  $x = L_1$  and  $x = L_2$  ( $L_2 > L_1$ ) leads us to most prototypical system in quantum mechanics: *particle in a box* (PIB). Application of such boundary condition invokes both quantization and confinement together in the form of an impenetrable box of length  $L = (L_2 - L_1)$  and energy  $\frac{n^2\pi^2}{2aL^2}$ . The eigenfunction of the  $n$ th state is expressed as  $\psi_n(x) = \sqrt{\frac{2}{L}} \sin\left(\frac{n\pi}{L}x\right)$ .



Let us consider a PIB with length  $L_m$ , whose  $m$ th state has the same energy with the  $n$ th state of another box with length  $L_n$ . Thus, one can write,

$$\begin{aligned}\frac{n^2\pi^2}{2aL_n^2} &= \frac{m^2\pi^2}{2aL_m^2} \\ \frac{n^2}{L_n^2} &= \frac{m^2}{L_m^2} \\ L_m &= \left(\frac{m}{n}\right) L_n.\end{aligned}\tag{17}$$

In PIB, a node at the point  $x_j$  appears when,  $\psi_n(x_j) = \sqrt{\frac{2}{L_n}} \sin\left(\frac{n\pi}{L_n}\right) x_j = 0$ . Therefore,

$$\begin{aligned}\sin\left(\frac{n\pi}{L_n}\right) x_j &= 0, \\ \text{thus, } x_j &= \left(\frac{m}{n}\right) L_n, \\ \text{finally, } L_m &= \left(\frac{m}{n}\right) L_n.\end{aligned}\tag{18}$$

Therefore, from Eqs. (17), and (18) we can conclude that, when  $n > m$  cases,  $L_m$  ( $m = 1, 2, 3, \dots$ ) are the nodal points of the  $n$ th state of the PIB having length  $L_n$ . Now, placing an impenetrable boundary at certain  $L_m$  value one can approach to isoenergetic states with energy  $\frac{n^2\pi^2}{2aL_n^2}$ . For, example, if  $m = 1$ , then  $n$  such state appears, similarly, for  $m = 2$ , we get,  $(n - 1)$  states. Obeying the same norm for  $m = m$  state provides  $(n - m + 1)$  number of states. Therefore, in completeness, for a given  $n$  we get  $\frac{n(n+1)}{2}$  number of incidental degenerate states. It is noteworthy to mention that, when  $m > n$ , then for each of the  $m$  values there arise an isoenergetic state with energy  $\frac{n^2\pi^2}{2aL_n^2}$  and box length  $L_m$ . But, they are not originated due to the incidental degeneracy condition, and for the sake of lucidness we call then additional degenerate states.

Thus, depending upon the value of  $m$ , two different types of degeneracy appear in PIB. Now, the point is to find out the answer, whether these degeneracies are appearing either due to quantization or due to confinement. In this context to determine the origin of these degeneracies, we invoke 1-Dimensional quantum harmonic oscillator (1-D QHO) having the form,  $v(x) = \frac{1}{2}\alpha^2 x^2$  ( $\alpha = 2\pi\nu$ ) and  $E_n = (n + \frac{1}{2})\alpha$ . Detailed analysis reveals that, in 1D QHO incidental degeneracy exists but not the accidental degeneracy. Thus, replacing the infinite barrier by a continuous potential would not hamper the incidental degeneracy (qualitative manner) in the system. Therefore, one can conjecture that, incidental degeneracy is a fundamental property of quantum systems and a consequence of quantization. However,

TABLE I: Incidental degeneracy in 1-D QHO associated with  $n = 1, 2$ .

Serial	No. of nodes	state ( $m$ )	$R_a$	$R_b$	Energy	1-D QHO state ( $n$ )
1a	0	0	$-\infty$	0	$\frac{3\alpha}{2}$	1
1b	0	0	0	$\infty$	$\frac{3\alpha}{2}$	1
1c	1	1	$-\infty$	$\infty$	$\frac{3\alpha}{2}$	1
2a	0	0	$-\infty$	$-\frac{1}{2\sqrt{\pi}}$	$\frac{5\alpha}{2}$	2
2b	0	0	$-\frac{1}{2\sqrt{\pi}}$	$\frac{1}{2\sqrt{\pi}}$	$\frac{5\alpha}{2}$	2
2c	0	0	$\frac{1}{2\sqrt{\pi}}$	$\infty$	$\frac{5\alpha}{2}$	2
2d	1	1	$-\infty$	$\frac{1}{2\sqrt{\pi}}$	$\frac{5\alpha}{2}$	2
2e	1	1	$-\frac{1}{2\sqrt{\pi}}$	$\infty$	$\frac{5\alpha}{2}$	2
2f	2	2	$-\infty$	$\infty$	$\frac{5\alpha}{2}$	2

additional degeneracy arises purely due to confinement. The total analysis in 1-D QHO is demonstrated in Table I involving  $n = 1, 2$  states ( $R_a, R_b$  are the nodal points of 1-D QHO. These are used to invoke shell confined condition.)

 TABLE II: Incidental degeneracy in DP and ECSCP, for  $\lambda_1, \lambda_2 = 200.0$  a.u.

Serial No.	Ref. state	Deg. state	No. of nodes	DP			ECSCP		
				$R_a$	$R_b$	Energy	$R_a$	$R_b$	Energy
2as	2s	1s	0	0	2.00009870	-0.12007414	0	2.0000026110	-0.12000171
2bs	2s	1s	0	2.00009870	100	-0.12007414	2.0000026110	100	-0.12000171
2cs	2s	2s	1	0	$\infty$	-0.12007414	0	$\infty$	-0.12000171
3as	3s	1s	0	0	1.902122031	-0.05072018	0	1.901934382	-0.05056383
3bs	3s	1s	0	1.9021220310	7.1008210	-0.05072018	1.901934382	7.09825460	-0.05056383
3cs	3s	1s	0	7.1008210	100	-0.05072018	7.09825460	100	-0.05056383
3ds	3s	2s	1	0	7.1008210	-0.05072018	0	7.09825460	-0.05056383
3es	3s	2s	1	1.9021220310	100	-0.05072018	1.901934382	100	-0.05056383
3fs	3s	3s	2	0	$\infty$	-0.05072018	0	$\infty$	-0.05056383
4as	4s	1s	0	0	1.8719797570	-0.02653747	0	1.87167478	-0.02627512
4bs	4s	1s	0	1.8719797570	6.614980540	-0.02653747	1.87167478	6.611235230	-0.02627512
4cs	4s	1s	0	6.614980540	15.54031890	-0.02653747	6.611235230	15.52028550	-0.02627512
4ds	4s	1s	0	15.54031890	100	-0.02653747	15.52028550	100	-0.02627512
4es	4s	2s	1	0	6.614980540	-0.02653747	0	6.611235230	-0.02627512
4fs	4s	2s	1	1.8719797570	15.54031890	-0.02653747	1.87167478	15.52028550	-0.02627512
4gs	4s	2s	1	6.614980540	100	-0.02653747	6.611235230	100	-0.02627512
4hs	4s	3s	2	0	15.54031890	-0.02653747	0	15.52028550	-0.02627512
4is	4s	3s	2	1.8719797570	100	-0.02653747	1.87167478	100	-0.02627512
4js	4s	4s	3	0	$\infty$	-0.02653747	0	$\infty$	-0.02627512
3ap	3p	2p	0	0	6.002624940	-0.05070822	0	6.000155460	-0.0505627661
3bp	3p	2p	0	6.002624940	100	-0.05070822	6.000155460	100	-0.0505627661
3cp	3p	3p	1	0	$\infty$	-0.05070822	0	$\infty$	-0.0505627661
4ap	4p	2p	0	0	5.531842190	-0.02652592	0	5.5282437020	-0.0262733156

*Continued on next page*

TABLE II – *Continued from previous page*

Serial No.	Ref. state	Deg. state	No. of nodes	DP			ECSCP		
				$R_a$	$R_b$	Energy	$R_a$	$R_b$	Energy
4bp	4p	2p	0	5.531842190	14.49475650	-0.02652592	5.5282437020	14.4747240030	-0.0262733156
4cp	4p	2p	0	14.49475650	100	-0.02652592	14.4747240030	100	-0.0262733156
4dp	4p	3p	1	0	14.49475650	-0.02652592	0	14.4747240030	-0.0262733156
4ep	4p	3p	1	5.531842190	100	-0.02652592	14.4747240030	100	-0.0262733156
4fp	4p	4p	2	0	$\infty$	-0.02652592	0	$\infty$	-0.0262733156
5ap	5p	2p	0	0	5.35879755	-0.015428340	0	5.3538548120	-0.0150560898
5bp	5p	2p	0	5.35879755	13.318341040	-0.015428340	5.3538548120	13.293465580	-0.0150560898
5cp	5p	2p	0	13.318341040	26.4658350	-0.015428340	13.293465580	26.378176830	-0.0150560898
5dp	5p	2p	0	26.4658350	100	-0.015428340	26.378176830	150	-0.0150560898
5ep	5p	3p	1	0	13.318341040	-0.015428340	0	13.293465580	-0.0150560898
5fp	5p	3p	1	5.35879755	26.4658350	-0.015428340	5.3538548120	26.378176830	-0.0150560898
5gp	5p	3p	1	13.318341040	150	-0.015428340	13.293465580	150	-0.0150560898
5hp	5p	4p	2	0	13.318341040	-0.015428340	0	26.378176830	-0.0150560898
5ip	5p	4p	2	5.35879755	150	-0.015428340	5.3538548120	150	-0.0150560898
5jp	5p	5p	3	0	$\infty$	-0.015428340	0	$\infty$	-0.0150560898
4ad	4d	3d	0	0	12.020605190	-0.0265028061	0	12.002149730	-0.026269684
4bd	4d	3d	0	12.020605190	100	-0.0265028061	12.002149730	200	-0.026269684
4cd	4d	4d	1	0	$\infty$	-0.0265028061	0	$\infty$	-0.026269684
5ad	5d	3d	0	0	10.91249580	-0.015406227	0	10.889614250	-0.015050727
5bd	5d	3d	0	10.91249580	24.2196030	-0.015406227	10.889614250	24.13278320	-0.015050727
5cd	5d	3d	0	24.2196030	150	-0.015406227	24.13278320	220	-0.015050727
5dd	5d	4d	1	0	24.2196030	-0.015406227	0	24.13278320	-0.015050727
5ed	5d	4d	1	10.91249580	150	-0.015406227	10.889614250	250	-0.015050727
5fd	5d	5d	2	0	$\infty$	-0.015406227	0	$\infty$	-0.015050727
6ad	6d	3d	0	0	10.46443610	-0.00947425	0	10.436313970	-0.008994213
6bd	6d	3d	0	10.46443610	22.08628590	-0.00947425	10.436313970	21.98896250	-0.008994213
6cd	6d	3d	0	22.08628590	39.9757030	-0.00947425	21.98896250	39.70523610	-0.008994213
6dd	6d	3d	0	39.9757030	125	-0.00947425	39.70523610	250	-0.008994213
6ed	6d	4d	1	0	22.08628590	-0.00947425	0	21.98896250	-0.008994213
6fd	6d	4d	1	10.46443610	39.9757030	-0.00947425	10.436313970	39.70523610	-0.008994213
6gd	6d	4d	1	22.08628590	150	-0.00947425	21.98896250	250	-0.008994213
6hd	6d	5d	2	0	22.08628590	-0.00947425	0	21.98896250	-0.008994213
6id	6d	5d	2	10.46443610	125	-0.00947425	10.436313970	250	-0.008994213
6kd	6d	6d	3	0	$\infty$	-0.00947425	0	$\infty$	-0.008994213

#### IV. RESULT AND DISCUSSION

Here we mention all four (FC, CS, SCC, LCS) models under the general heading of GCS. However, since the energy characteristics of these models are quite different. Demonstrative results are reported for both DP and ECSCP ( $Z = 1$ ). However, analogous results can be

found for  $Z \neq 1$  cases. At the onset, we discuss several salient features of incidental degeneracy obtained by placing the boundary at respective nodal positions of DP and ECSCP in both *free* and *confined* situations. Next, we report  $f^{(k)}(Z)$  and  $\alpha^{(k)}(Z)$  ( $k = 1$ ) for some low-lying states of DP and ECSCP, involving FC, CS, SCC models. Further, we have evaluated  $\alpha^{(1)}(Z)$  for  $1s, 2s, 2p, 3s, 3d, 4s$  states. It is necessary to point out that, in case of degeneracy, radial boundaries are opted specifically at the nodes of DP/ECSCP to demonstrate their role. Whereas for  $f^{(k)}, \alpha^{(k)}$ , no such condition was taken into consideration. Further, it may be noted that, for either of the plasmas (DP and ECSCP), all these calculations are performed in the range of  $\lambda$  between 0 – 200 a.u. Here we report results involving  $\lambda = 200$  a.u. Because, at this  $\lambda$  values higher number of bound states exists in DP and ECSCP. Pilot calculations are executed in two steps. At first we investigate incidental degeneracy and spectroscopic properties for DP and ECSCP. Later, we look into the effect of external electric field on incidental degeneracy, dipole oscillator strength and polarizability.

### A. Incidental Degeneracy

Following [88], it is a well known fact that, if  $R_a, R_b$  of a *Generalized confined hydrogen atom* (GCHA) [71] merge with certain specific radial nodes of  $(n, \ell)$  state of *free H-atom* (FHA), as a result there exists  $(n' - \ell - 1)$  number of nodes in between them. Moreover, energy of such a  $(n', \ell)$  GCHA state appears to be degenerate to that of a FHA state. Equation (3) depicts that, *shell confined* condition introduces four different systems. This degeneracy proposes the inter-connection amongst them. Here, we involve ourselves to investigate the same for plasma systems in both *confined* and *free* conditions, where the systems are devoid of *accidental degeneracy*. Further, we would also determine the number of *degenerate states* attached with a given plasma energy in either of the potentials. It should also be keep in mind that, the conclusions for *free* DP and ECSCP are drawn assuming the existence of infinite number of bound states in them. However, with decrease in bound states, number of such degenerate states reduces.

TABLE III: Incidental degeneracy in *confined* DP and ECSCP ( $r_c = 5$  a.u.),  
for  $\lambda_1, \lambda_2 = 200.0$  a.u.

Serial No.	Ref. state	Deg. state	No. of nodes	DP			ECSCP		
				$R_a$	$R_b$	Energy	$R_a$	$R_b$	Energy
2as	2s	1s	0	0	1.6982037372	0.1462201782	0	1.69818325927	0.14625383593
2bs	2s	1s	0	1.6982037372	5	0.1462201782	1.69818325927	5	0.14625383593
2cs	2s	2s	1	0	5	0.1462201782	0	5	0.14625383593
3as	3s	1s	0	0	1.2580446107	1.0581877266	0	1.258034184915	1.05822024961
3bs	3s	1s	0	1.2580446107	3.0543621890	1.0581877266	1.258034184915	3.054349992880	1.05822024961
3cs	3s	1s	0	3.0543621890	5	1.0581877266	3.054349992880	5	1.05822024961
3ds	3s	2s	1	0	3.0543621890	1.0581877266	0	3.054349992880	1.05822024961
3es	3s	2s	1	1.2580446107	5	1.0581877266	1.258034184915	5	1.05822024961
3fs	3s	3s	2	0	3.0543621890	1.0581877266	0	5	1.05822024961
4as	4s	1s	0	0	0.99888647574	2.3872929368	0	0.998882989430	2.38732482829
4bs	4s	1s	0	0.99888647574	2.28016476628	2.3872929368	0.998882989430	2.280158398620	2.38732482829
4cs	4s	1s	0	2.28016476628	3.62627582410	2.3872929368	2.280158398620	3.626270386398	2.38732482829
4ds	4s	1s	0	3.62627582410	5	2.3872929368	3.626270386398	5	2.38732482829
4es	4s	2s	1	0	2.28016476628	2.3872929368	0	2.280158398620	2.38732482829
4fs	4s	2s	1	0.99888647574	3.62627582410	2.3872929368	0.998882989430	3.626270386398	2.38732482829
4gs	4s	2s	1	2.28016476628	5	2.3872929368	2.280158398620	5	2.38732482829
4hs	4s	3s	2	0	3.62627582410	2.3872929368	0	3.626270386398	2.38732482829
4is	4s	3s	2	0.99888647574	5	2.3872929368	0.998882989430	5	2.38732482829
4js	4s	4s	3	0	5	2.3872929368	0	5	2.38732482829
3ap	3p	2p	0	0	2.66019090630	0.712685104711	0	2.66017318418	0.7127180559
3bp	3p	2p	0	2.66019090630	5	0.712685104711	2.66017318418	5	0.7127180559
3cp	3p	3p	1	0	5	0.712685104711	0	5	0.7127180559
4ap	4p	2p	0	0	1.887659760260	1.835390736624	0	1.887652169531	1.835423002175
4bp	4p	2p	0	1.887659760260	3.43376514750	1.835390736624	1.887652169531	3.43375766692	1.835423002175
4cp	4p	2p	0	3.43376514750	5	1.835390736624	3.43375766692	5	1.835423002175
4dp	4p	3p	1	0	3.4337651475	1.835390736624	0	3.43375766692	1.835423002175
4ep	4p	3p	1	1.887659760260	5	1.835390736624	1.887652169531	5	1.835423002175
4fp	4p	4p	2	0	5	1.835390736624	0	5	1.835423002175
5ap	5p	2p	0	0	1.475168797140	3.367619082432	0	1.475164887123	3.367650934911
5bp	5p	2p	0	1.475168797140	2.644363878450	3.367619082432	1.475164887123	2.644358936263	3.367650934911
5cp	5p	2p	0	2.644363878450	3.819016714020	3.367619082432	2.644358936263	3.819013041801	3.367650934911
5dp	5p	2p	0	3.819016714020	5	3.367619082432	3.819013041801	5	3.367650934911
5ep	5p	3p	1	0	2.644363878450	3.367619082432	0	2.644358936263	3.367650934911
5fp	5p	3p	1	1.475168797140	3.819016714020	3.367619082432	1.475164887123	3.819013041801	3.367650934911
5gp	5p	3p	1	2.644363878450	5	3.367619082432	2.644358936263	5	3.367650934911
5hp	5p	4p	2	0	3.819016714020	3.367619082432	0	3.819013041801	3.367650934911
5ip	5p	4p	2	1.475168797140	5	3.367619082432	1.475164887123	5	3.367650934911
5jp	5p	5p	3	0	5	3.367619082432	0	5	3.367650934911
4ad	4d	3d	0	0	3.05208227850	1.244615818343	0	3.052071249402	1.244650639470
4bd	4d	3d	0	3.05208227850	5	1.244615818343	3.052071249402	5	1.244650639470
4cd	4d	4d	1	0	5	1.244615818343	0	5	1.244650639470

Continued on next page

TABLE III – *Continued from previous page*

Serial No.	Ref. state	Deg. state	No. of nodes	DP			ECSCP		
				$R_a$	$R_b$	Energy	$R_a$	$R_b$	Energy
5ad	5d	3d	0	0	2.24218003190	2.572144022112	0	2.242174038040	2.57217744067
5bd	5d	3d	0	2.24218003190	3.63202185420	2.572144022112	2.242174038040	3.632016812010	2.57217744067
5cd	5d	3d	0	3.63202185420	5	2.572144022112	3.63201681201	5	2.57217744067
5dd	5d	4d	0	0	3.63202185420	2.572144022112	0	2.24217403804	2.57217744067
5ed	5d	4d	0	2.24218003190	3.63202185420	2.572144022112	3.63201681201	5	2.57217744067
5fd	5d	5d	0	0	5	2.572144022112	0	5	2.57217744067
6ad	6d	3d	0	0	1.78281220402	4.306287086796	0	1.782814849720	4.306319753147
6bd	6d	3d	0	1.78281220402	2.870891048410	4.306287086796	1.782814849720	2.870897278402	4.306319753147
6cd	6d	3d	0	2.870891048410	3.937869825880	4.306287086796	2.870897278402	3.93788113360	4.306319753147
6dd	6d	3d	0	3.937869825880	5	4.306287086796	3.93788113360	5	4.306319753147
6ed	6d	4d	1	0	2.870891048410	4.306287086796	0	2.870897278402	4.306319753147
6fd	6d	4d	1	1.78281220402	3.937869825880	4.306287086796	1.782814849720	3.93788113360	4.306319753147
6gd	6d	4d	1	2.870891048410	5	4.306287086796	2.870897278402	5	4.306319753147
6hd	6d	5d	2	0	3.937869825880	4.306287086796	0	3.93788113360	4.306319753147
6id	6d	5d	2	1.78281220402	5	4.306287086796	1.782814849720	5	4.306319753147
6kd	6d	6d	3	0	5	4.306287086796	0	5	4.306319753147

In both DP and ECSCP number of bound states reduces with decrease in  $\lambda$  values. Thus, it is more pertinent to examine the *incidental degeneracy* in plasma systems. Table II, renders the incidental degeneracy for *free* DP and ECSCP, taking (a)  $n = 2 - 4$  in  $s$  states ( $\ell = 0$ ), (b)  $n = 3 - 5$  in  $p$  states ( $\ell = 1$ ), and (c)  $n = 4 - 6$  in  $d$  states ( $\ell = 2$ ), successively. Just to remind that,  $R_a, R_b$  are chosen to be the nodal points of respective  $s, p, d$  states in *free* plasmas. In DP, at  $n = 2, \ell = 0$  (energy =  $-0.12007414$  a.u.), a three fold degeneracy exists with one confined ( $2as$ ), one left-confined ( $2bs$ ) and one free ( $2cs$ ) DP. Further, (a)  $n = 3, \ell = 1$  (energy =  $-0.05070822$  a.u.) and (b)  $n = 4, \ell = 2$  (energy =  $-0.0265028061$ ) states are three fold degenerate with one CS ( $3ap$  or  $4ad$ ), one LCS ( $3bp$  or  $4bd$ ) and one FC ( $3cp$  or  $4cd$ ) respectively. This degeneracy in *shell-confined* DP involving  $s, p, d$  states, however arises at  $n = 3, 4, 5$  consecutively with energies  $\epsilon_{3s} = -0.0572018$  a.u.,  $\epsilon_{4p} = -0.02652592$  a.u. and  $\epsilon_{5d} = -0.015406227$  a.u. In each of these three cases, there survives six degenerate states in DP, namely, confined ( $3as, 3ds$  or  $4ap, 4dp$  or  $5ad, 5dd$ ), shell-confined ( $3bs$  or  $4bp$  or  $5bd$ ), left-confined ( $3cs, 3es$  or  $4cp, 4ep$  or  $5cd, 5ed$ ) and free ( $3fs$  or  $4fp$  or  $5fd$ ) DP. The incidental degeneracy in a *shell-confined*  $\ell$ -state in DP appears at  $n = (\ell + 3)$ . Further, for each of the following  $4s$  ( $\epsilon_{4s} = -0.02653747$  a.u.) or  $5p$  ( $\epsilon_{5p} = -0.015428340$  a.u.) or  $6d$  ( $\epsilon_{6d} = -0.00947425$  a.u.) states there are ten degenerate states belonging to confined ( $4as, 4es, 4hs$  or  $5ap, 5ep, 5hp$  or  $6ad, 6ed, 6hd$ ), shell-confined

( $4bs, 4cs, 4fs$  or  $5bp, 5cp, 5fp$  or  $6bd, 6cd, 6fd$ ), left-confined ( $4ds, 4gs, 4is$  or  $5dp, 5gp, 5ip$  or  $6dd, 6gd, 6id$ ) and free ( $4js$  or  $5jp$  or  $6jd$ ) DP respectively. Now moving to ECSCP system, one experiences exactly identical degeneracy pattern as DP, with explicit energy difference between the two. Barring an example we can mention that, akin to DP, in ECSCP such degeneracy involving a *shell-confined*  $\ell$ -state arises at  $n = (\ell + 3)$ . Therefore, one can aptly conjecture that, irrespective of the plasmas, incidental degeneracy for a given *shell-confined*  $\ell$ -state arrives at  $n = (\ell + 3)$ .

TABLE IV: Incidental degeneracy in *confined* DP and ECSCP under *external electric field*, for  $\lambda_1, \lambda_2 = 200.0$  a.u. and  $F=0.1$  a.u.

Serial No.	Ref. state	Deg. state	No. of nodes	DP			ECSCP		
				$R_a$	$R_b$	Energy	$R_a$	$R_b$	Energy
2as	2s	1s	0	0	1.63122916140	0.30421477724	0	1.63120322910	0.29925846975
2bs	2s	1s	0	1.63122916140	120	0.30421477724	1.63120322910	125	0.29925846975
2cs	2s	2s	1	0	$\infty$	0.30421477724	0	$\infty$	0.29925846975
3as	3s	1s	0	0	1.430987056806	0.64608902466	0	1.430960046710	0.64115528522
3bs	3s	1s	0	1.430987056806	3.98416222870	0.64608902466	1.430960046710	3.98405258470	0.64115528522
3cs	3s	1s	0	3.98416222870	150	0.64608902466	3.98405258470	125	0.64115528522
3ds	3s	2s	1	0	3.98416222870	0.64608902466	0	3.98405258470	0.64115528522
3es	3s	2s	1	1.430987056806	150	0.64608902466	1.430960046710	150	0.64115528522
3fs	3s	3s	2	0	$\infty$	0.64608902466	0	$\infty$	0.64115528522
4as	4s	1s	0	0	1.323704568110	0.91194766539	0	1.323677129230	0.90703311507
4bs	4s	1s	0	1.323704568110	3.437749731312	0.91194766539	1.323677129230	3.43765212650	0.90703311507
4cs	4s	1s	0	3.437749731312	6.2231958170	0.91194766539	3.43765212650	6.22299514840	0.90703311507
4ds	4s	1s	0	6.2231958170	150	0.91194766539	6.22299514840	125	0.90703311507
4es	4s	2s	1	0	3.437749731312	0.91194766539	0	3.43765212650	0.90703311507
4fs	4s	2s	1	1.323704568110	6.2231958170	0.91194766539	1.323677129230	6.22299514840	0.90703311507
4gs	4s	2s	1	3.437749731312	150	0.91194766539	3.43765212650	150	0.90703311507
4hs	4s	3s	2	0	6.2231958170	0.91194766539	0	6.22299514840	0.90703311507
4is	4s	3s	2	1.323704568110	180	0.91194766539	1.323677129230	150	0.90703311507
4js	4s	4s	3	0	$\infty$	0.91194766539	0	$\infty$	0.90703311507
3ap	3p	2p	0	0	3.1735238880	0.57546550714	0	3.17343008710	0.57052461177
3bp	3p	2p	0	3.1735238880	150	0.57546550714	3.1734300871	125	0.57052461177
3cp	3p	3p	1	0	$\infty$	0.57546550714	0	$\infty$	0.57052461177
4ap	4p	2p	0	0	2.6815598797	0.84563053412	0	2.68147834530	0.84070941159
4bp	4p	2p	0	2.6815598797	5.5042196423	0.84563053412	2.68147834530	5.50403433220	0.84070941159
4cp	4p	2p	0	5.5042196423	180	0.84563053412	5.50403433220	125	0.84070941159
4dp	4p	3p	1	0	5.5042196423	0.84563053412	0	5.50403433220	0.84070941159
4ep	4p	3p	1	2.6815598797	180	0.84563053412	2.68147834530	150	0.84070941159
4fp	4p	4p	2	0	$\infty$	0.84563053412	0	$\infty$	0.84070941159
5ap	5p	2p	0	0	2.41957855790	1.0779685915	0	2.419503441880	1.0730649761
5bp	5p	2p	0	2.41957855790	4.73787060730	1.0779685915	2.419503441880	4.737710002070	1.0730649761

Continued on next page

TABLE IV – *Continued from previous page*

Serial No.	Ref. state	Deg. state	No. of nodes	DP			ECSCP		
				$R_a$	$R_b$	Energy	$R_a$	$R_b$	Energy
5cp	5p	2p	0	4.73787060730	7.6216242920	1.0779685915	4.737710002070	7.6213531670	1.0730649761
5dp	5p	2p	0	7.6216242920	200	1.0779685915	7.6213531670	150	1.0730649761
5ep	5p	3p	1	0	4.73787060730	1.0779685915	0	4.737710002070	1.0730649761
5fp	5p	3p	1	2.41957855790	7.6216242920	1.0779685915	2.419503441880	7.6213531670	1.0730649761
5gp	5p	3p	1	4.73787060730	200	1.0779685915	4.737710002070	160	1.0730649761
5hp	5p	4p	2	0	7.6216242920	1.0779685915	0	7.6213531670	1.0730649761
5ip	5p	4p	2	2.41957855790	200	1.0779685915	2.419503441880	180	1.0730649761
5jp	5p	5p	3	0	$\infty$	1.0779685915	0	$\infty$	1.0730649761
4ad	4d	3d	0	0	4.37176436570	0.76153364255	0	4.371614629150	0.7566050503
4bd	4d	3d	0	4.37176436570	200	0.76153364255	4.371614629150	130	0.7566050503
4cd	4d	4d	1	0	$\infty$	0.76153364255	0	$\infty$	0.7566050503
5ad	5d	3d	0	0	3.6994249718	0.99951100719	0	3.6992974680	0.99460049179
5bd	5d	3d	0	3.6994249718	6.676090403	0.99951100719	3.6992974680	6.675849412170	0.99460049179
5cd	5d	3d	0	6.676090403	200	0.99951100719	6.675849412170	180	0.99460049179
5dd	5d	4d	0	0	6.676090403	0.99951100719	0	6.675849412170	0.99460049179
5ed	5d	4d	0	3.6994249718	200	0.99951100719	3.6992974680	200	0.99460049179
5fd	5d	5d	0	0	$\infty$	0.99951100719	0	$\infty$	0.99460049179
6ad	6d	3d	0	0	3.3301902855	1.21275230925	0	3.3300747810	1.2078581777
6bd	6d	3d	0	3.33019028550	5.77461618903	1.21275230925	3.3300747810	5.7744075560	1.2078581777
6cd	6d	3d	0	5.774616189030	8.72983376980	1.21275230925	5.7744075560	8.7295104230	1.2078581777
6dd	6d	3d	0	8.72983376980	200	1.21275230925	8.7295104230	180	1.2078581777
6ed	6d	4d	1	0	5.77461618903	1.21275230925	0	5.7744075560	1.2078581777
6fd	6d	4d	1	3.33019028550	8.72983376980	1.21275230925	3.3300747810	8.7295104230	1.2078581777
6gd	6d	4d	1	5.774616189030	200	1.21275230925	5.7744075560	180	1.2078581777
6hd	6d	5d	2	0	8.72983376980	1.21275230925	0	8.7295104230	1.2078581777
6id	6d	5d	2	3.33019028550	200	1.21275230925	3.3300747810	200	1.2078581777
6kd	6d	6d	3	0	$\infty$	1.21275230925	0	$\infty$	1.2078581777

At this point, we aim to verify the impact of high pressure and external electric field on such degeneracy pattern in DP and ECSCP. Table III, imprints the incidental degeneracy for *confined* DP and ECSCP at  $r_c = 5$  a.u., for  $2s, 3s, 4s, 3p, 4p, 5p, 4d, 5d, 6d$  states. As usual,  $R_a, R_b$  are fixed at the nodal points of successive  $s, p, d$  orbitals in *confined* plasmas. Similarly, Table IV displays the same for DP and ECSCP under the impression of external electric field ( $F \cos \theta = 0.1$  a.u.). Detailed analysis reveals that, in high pressure condition and in external electric field one encounters exactly uniform pattern of degeneracy as their respective *free* counterpart, with obvious change in energy between them. Therefore, incidental degeneracy remains unaffected with these two external effects. This again promptly asserts the implicitness of this degeneracy.



Now, analyzing Tables II-IV, it can be extracted that, there arises  $\frac{(n-\ell)(n-\ell+1)}{2}$  number of degenerate states in GCS. Therefore, for a certain  $n$ -state of DP or ECSCP, the total count of GCS states becomes,  $\frac{(n-\ell)(n-\ell+1)}{2}$ . It suggests that, this number depends on both  $n, \ell$  quantum numbers. Now, we can, calculate the contribution of each of these four systems in this degeneracy, as given below.

- (I) **FC:** At a given  $(n, \ell)$ -state, there exists only one energy states.
- (II) **CS:** An  $(n, \ell)$ -orbital contributes  $(n - \ell - 1)$  number of degenerate states.
- (III) **SCC:**  $(n, \ell)$ -state contributes as  $\frac{(n-\ell-2)(n-\ell-1)}{2}$ .
- (IV) **LCS:** A particular  $(n, \ell)$  orbital contributes  $(n - \ell - 1)$  degenerate states.

In confined plasmas, LCS modifies to SCS with  $R_b$  is kept fixed at a certain value. Thus, SCC contributes,

$$\begin{aligned}
 & \frac{(n - \ell - 1)(n - \ell - 2)}{2} + (n - \ell - 1) \\
 &= (n - \ell - 1) \left[ 1 + \frac{(n - \ell - 2)}{2} \right] \\
 &= \frac{(n - \ell)(n - \ell - 1)}{2}.
 \end{aligned} \tag{19}$$

On the basis of above discussion and Tables II-IV, one can trace out certain characteristics. In order to simplify, we mention  $n, \ell$  to refer principal and orbital quantum number of *free* plasmas, whereas  $n_k, \ell_j$  indicates the same for other three systems ( $k, j$  are integers).

- (i) Each  $\ell$ -state having fixed  $n$  value, contributes  $\frac{(n-\ell)(n-\ell+1)}{2}$  number of GCS states.
- (ii) At a certain  $\ell$  the count of such degenerate state increases with  $n$ . On the contrary, at a certain  $n$ , the number of degenerate states reduce with rise in  $\ell$ .
- (iii) In SCC degeneracy appears at  $n = 3$ .
- (iv) Two arbitrary states  $(n_1, \ell_1), (n_2, \ell_2)$  become degenerate when  $n_1 < n, \ell_1 < n$  and  $n_2 < n, \ell_2 < n$ . They may be associated to any of the systems in GCS, except FC.

Apart from the incidental degeneracy, here we point out the existence of another degeneracy in confined plasmas ( $R_a = 0$ ). Table V, exhibit such degeneracy pattern in confined DP and ECSCP involving  $1s$  state. At  $R_b = 1$ , the energy ( $\epsilon_{1s} = 2.3789850177$ )

TABLE V: Additional degeneracy in *confined* DP and ECSCP, for  $\lambda_1, \lambda_2 = 200$  a.u.

		DP		ECSCP			
Serial No.	State	$R_a$	$R_b$	Energy	$R_a$	$R_b$	Energy
1	1s	0	1	2.3789850177	0	1	2.3789908559
2	2s	0	2.2832202233	2.3789850177	0	2.2832234381	2.3789908559
3	2p	0	1.7024233032	2.3789850177	0	1.7024251301	2.3789908559
4	3s	0	3.6315075428	2.3789850177	0	3.6315185462	2.3789908559
5	3p	0	3.0758583379	2.3789850177	0	3.0758664112	2.3789908559
6	3d	0	2.3198593110	2.3789850177	0	2.3198645970	2.3789908559
7	4s	0	5.0075095717	2.3789850177	0	5.0075332221	2.3789908559
8	4p	0	4.4617689881	2.3789850177	0	4.4617880726	2.3789908559
9	4d	0	3.7617324892	2.3789850177	0	3.7617470592	2.3789908559
10	4f	0	2.9013975139	2.3789850177	0	2.9014076831	2.3789908559
..	..	..	..	..	..	..	..
..	..	..	..	..	..	..	..
1	1s	0	2	-0.1200107236	0	2	-0.12000003625
2	2s	0	17.9007405190	-0.1200107236	0	22.5883720000	-0.12000003625
3	2p	0	17.0684450000	-0.1200107236	0	21.8984020000	-0.12000003625
1	1s	0	3	-0.4189816690	0	3	-0.418967355112

of 1s-state becomes degenerate with 2s ( $R_b = 2.2832202233$ ), 2p ( $R_b = 1.7024233032$ ), 3s ( $R_b = 3.6315075428$ ), ..., 4f ( $R_b = 2.9013975139$ ), and so on. At, this  $R_a$  value,  $\epsilon_{1s}$  is positive and greater than  $\epsilon_{n,\ell}^{free}$ . Here,  $\epsilon_{n,\ell}^{free}$  represent the energy of the  $(n, \ell)$  state in absence of pressure. However, at  $R_b = 2$ , 1s-state ( $\epsilon_{1s} = -0.1200107236$ ) is degenerate with only 2s ( $R_b = 17.9007405190$ ) and 2p ( $R_b = 17.0684450000$ ) states. It happens because at  $R_b = 2$ ,  $\epsilon_{1s}$  is only higher than the energy of  $\epsilon_{2s}^{free}, \epsilon_{2p}^{free}$ . Finally, at  $R_b = 3$ ,  $\epsilon_{1s}$  becomes non-degenerate. Similar observation can also be obtain for excited states. In essence it can be stated that, when  $\epsilon_{1s} > 0$ , then there exists infinite number of such degenerate states. However, when  $\epsilon_{1s} < 0$  region, with decrease in energy value count of such degenerate state declines. After a certain limiting value, it becomes non degenerate. This type of degeneracy occurs only in confined systems and the count of such degenerate state complete depends on the strength of confinement. With increase in pressure, the energy of 1s-state increases, as consequence number of degenerate state increases. More importantly, here we have presented the results for 1s-state. However, similar observation can also be recorded for an arbitrary bound state.

TABLE VI:  $f^{(1)}$  involving  $1s, 2s, 2p$  states in *confined* DP and ECSCP for  $\lambda_1, \lambda_2 = 200$  a.u.

		DP							
$R_a$	$R_b$	$1s \rightarrow 2p$	$1s \rightarrow 3p$	$2s \rightarrow 2p$	$2s \rightarrow 3p$	$2p \rightarrow 1s$	$2p \rightarrow 2s$	$2p \rightarrow 3d$	$2p \rightarrow 4d$
0	1	0.9845583736	0.007725936	-0.6082578489	1.5603265067	-0.3281861245	0.2027526163	1.084824819	0.018576821
0.1	1	0.8991021968	0.091177999	-0.5487515200	1.2675987342	-0.2997007322	0.1829171733	1.078261447	0.025793358
0.2	1	0.8115882841	0.176644625	-0.4643464211	1.0121522214	-0.2705294280	0.1547821403	1.044480208	0.059665545
0.5	1	0.6974611899	0.289644039	-0.3508420476	0.7344790098	-0.2324870633	0.1169473492	0.929550287	0.173160326
0.8	1	0.6699145798	0.316999576	-0.3234507070	0.6737046104	-0.2233048599	0.1078169023	0.893218984	0.209183954
0	5	0.8488024520	0.108272180	-0.4563748356	1.4233367326	-0.2829341506	0.1521249452	1.103032718	0.001023063
0.5	5	0.93301292953	0.053537177	-0.5865015753	1.3312315839	-0.3110043098	0.1955005251	1.097736184	0.008041007
1	5	0.82132893350	0.164523624	-0.4739305826	1.0274313977	-0.2737763111	0.1579768608	1.106595561	0.000413399
2	5	0.72015045177	0.266781857	-0.3732478855	0.7855584038	-0.2400501505	0.1244159618	0.958259417	0.144671064
3	5	0.68357364638	0.303403595	-0.3370006030	0.7035722963	-0.2278578821	0.1123335343	0.911368314	0.191162267
4.5	5	0.66739177323	0.319504855	-0.3209450048	0.6682356487	-0.2224639244	0.1069816682	0.889855689	0.212523233
0	10	0.49197804318	0.258217079	-0.0777278384	0.9674872235	-0.1639926810	0.0259092794	1.070082794	0.027997652
0.5	10	0.97045011671	0.014376086	-0.6209901235	1.5633135494	-0.3234833722	0.2069967078	1.086251699	0.016845793
1	10	0.94768087310	0.024025469	-0.5899418568	1.3674404123	-0.3158936243	0.1966472856	1.106595561	0.000413399
3	10	0.75955594681	0.224597411	-0.4104142965	0.8749891665	-0.2531853156	0.1368047655	1.004384636	0.098397827
5	10	0.69774049664	0.289034898	-0.3508574954	0.7348647740	-0.2325801655	0.1169524984	0.929957661	0.172609822
7.5	10	0.67206042643	0.314861162	-0.3255754666	0.6783672042	-0.2240201421	0.1085251555	0.896078528	0.206340948
9.5	10	0.66683857872	0.320054255	-0.3203956825	0.6670385359	-0.2222795262	0.1067985608	0.889118104	0.213255697
		ECSCP							
$R_a$	$R_b$	$1s \rightarrow 2p$	$1s \rightarrow 3p$	$2s \rightarrow 2p$	$2s \rightarrow 3p$	$2p \rightarrow 1s$	$2p \rightarrow 2s$	$2p \rightarrow 3d$	$2p \rightarrow 4d$
0	1	0.9845583944	0.0077259195	-0.6082578857	1.5603265595	-0.3281861314	0.2027526285	1.084824835	0.018576809
0.1	1	0.8991022160	0.0911779811	-0.5487515470	1.2675987702	-0.2997007386	0.1829171823	1.078261461	0.025793346
0.2	1	0.8115882910	0.1766446184	-0.4643464305	1.0121522331	-0.2705294303	0.1547821435	1.044480217	0.059665537
0.5	1	0.6974611901	0.2896440393	-0.3508420478	0.7344790100	-0.2324870633	0.1169473492	0.929550287	0.173160326
0.8	1	0.6699145791	0.3169995763	-0.3234507070	0.6737046103	-0.2233048597	0.1078169023	0.893218984	0.209183954
0	5	0.8487992934	0.1082749684	-0.4563746338	1.4233366775	-0.2829330978	0.1521248779	1.103033440	0.001022600
0.5	5	0.9330138952	0.0535357427	-0.5865027973	1.3312341111	-0.3110046317	0.1955009324	1.097737370	0.008040088
1	5	0.7201505110	0.2667817486	-0.4739309943	1.0274323378	-0.2737764770	0.1579769981	1.055607457	0.049069981
2	5	0.6835736500	0.3034035886	-0.3732479200	0.7855585007	-0.2400501703	0.1244159733	0.958259517	0.144670958
3	5	0.6835736500	0.3034035886	-0.3370006045	0.7035723022	-0.2278578833	0.1123335348	0.911368319	0.191162261
4.5	5	0.6673917703	0.3195048550	-0.3209450048	0.6682356472	-0.2224639234	0.1069816682	0.889855688	0.212523233
0	10	0.492037585	0.2581751997	-0.0778155020	0.9675474065	-0.1640125285	0.0259385006	1.070064435	0.028015562
0.5	10	0.970452919	0.0143709867	-0.6209863259	1.5633183645	-0.3234843064	0.2069954419	1.086240012	0.016858413
1	10	0.947674297	0.0240247854	-0.5899250652	1.3674340783	-0.3158914323	0.1966416884	1.106595224	0.000414800
3	10	0.759556484	0.2245945414	-0.4104128653	0.8749903496	-0.2531854949	0.1368042884	1.004386314	0.098395452
5	10	0.697740596	0.2890345618	-0.3508574039	0.7348649380	-0.2325801989	0.1169524679	0.929957822	0.172609559
7.5	10	0.672060427	0.3148611579	-0.3255754655	0.6783672047	-0.2240201425	0.1085251551	0.896078529	0.206340945
9.5	10	0.666838573	0.3200542553	-0.3203956826	0.6670385259	-0.2222795243	0.1067985608	0.889118103	0.213255697

## B. Multipole oscillator strength and polarizability

This section is divided into two parts. At first we report  $f^{(1)}$  and  $\alpha^{(1)}$  for confined DP and ECSCP, in some low-lying states. Finally, we discuss the impact of external electric field on  $f^{(1)}$  and  $\alpha^{(1)}$  for these two confined plasmas. Except  $f^{(1)}, \alpha^{(1)}$  of  $1s, 2s$  in confined DP and ECSCP, no results are presented so far in any of the GCS plasmas [10]. Coincidentally, that calculations are performed by the present author using GPS method. However, the impact of external electric field on these  $f^{(1)}, \alpha^{(1)}$  are not been reported before. As a consequence, no such literature is available for comparison.

At the beginning, we point out that, the oscillator strength sum rule, Eq. (13) is obeyed by all states in confined DP and ECSCP.  $f^{(k)}$  measures the probability of transition from an initial to final state. It is the ratio involving the quantum mechanical transition rate and the classical absorption/emission rate connecting a single electron oscillator having same frequency of transition. It is a dimensionless quantity. It becomes  $-ve$  for emission and  $+ve$  for absorption. Further, an emissive state with small value of oscillator strength explains that, non-radiative decay outpaces radiative decay [? ].

The selection rule for dipole transition is,  $\Delta\ell = \pm 1$ . As a consequence, from an  $s$  state, transition is only possible to a  $p$  state. But from  $p$  state, transition may takes place to  $\ell = 0, 2$  states. Table VI demonstrates estimated  $f^{(1)}$  for  $1s, 2s, 2p$  involving  $n, \ell \rightarrow n', (\ell+1)$  ( $n = 1, 2; n' = 2, 3, 4$ ) transitions involving DP and ECSCP. In either of the plasmas, SCC outcomes are presented for three  $R_b$ , namely, 1, 5, 10; for each  $R_b$ ,  $R_a$  changes from  $0 - R_b$ . Here, CS situation is achieved at  $R_a = 0$ , consequently,  $r_c = R_b = 1, 5, 10$ .  $f_{1s \rightarrow 2p}^{(1)}$  in both confined DP and ECSCP decreases with rise in  $r_c$  to merge to respective free values. In *shell-confined* condition, for  $R_b = 1$  it declines with progress in  $R_a$ . At  $R_b = 5, 10$  it increases to reach a maximum then decreases. The behavior of  $f_{1s \rightarrow 3p}^{(1)}$  is distinctly different from  $f_{1s \rightarrow 2p}^{(1)}$ . In confined DP and ECSCP completely opposite trend is observed— it increases with advancement of  $r_c$  to converge to their free limits. In SCC, at  $R_b = 1$ , it advances with  $R_a$ . However, at  $R_b = 5, 10$  it declines to reach a minimum then increases.  $f_{2s \rightarrow 2p}^{(1)}$  is always ( $-ve$ ), which indicates that, except *free* plasmas, the former has higher energy than latter. At  $R_a = 0$ , its absolute value abates with progress in  $r_c = R_b$ . Interestingly in SCC, at  $R_b = 1$ , its magnitude decreases with enhancement of  $R_a$ . Beside this, at  $R_b = 5, 10$ , its absolute value increases to climb a maximum then declines with growth in  $R_a$ . For  $f_{2s \rightarrow 3p}^{(1)}$

transition,  $f^{(1)}$  in *confined* plasmas declines with progress in  $r_c$  to convene to their free values. Further, at  $R_b = 1, 5$ , it again abates with rise in  $R_a$ . Conversely, at  $R_b = 10$ , it attains a maximum then decreases. Similar to  $f^{(1)}$  in  $2s \rightarrow 2p$  transition,  $f_{2p \rightarrow 1s}^{(1)}$  is always  $-ve$ . Moreover, in both *confined* and *shell-confined* plasmas it portrays exactly identical pattern to  $f_{2s \rightarrow 2p}^{(1)}$ . Although they possesses different numerical values. In case of  $2p \rightarrow 2s$  transition,  $f^{(1)}$  decreases with rise in  $r_c$ . However, in SCC, it imprints similar behavior to  $f_{1s \rightarrow 3p}^{(1)}$ . Now, for  $f_{2p \rightarrow 3d}^{(1)}$ , in CS we observe a maximum. It is noteworthy to mention that, in SCC, it imprints similar pattern to  $1s \rightarrow 3p$  transition. Importantly, in *confined* plasmas  $f_{2p \rightarrow 4d}^{(1)}$  behaves exactly reverse to  $f_{2p \rightarrow 3d}^{(1)}$ . Further, in *shell-confined* situation, at  $R_b = 1, 5$ , it advances with rise in  $R_a$ . On the contrary, at  $R_b = 10$ , it falls off to a minimum then increases.

Now we move to investigate  $\alpha^{(1)}$  in *confined* and *shell-confined* plasmas by means of sample calculations on  $1s, 2s, 2p, 3s, 3p, 3d, 4s$  states. In case of  $p$  and  $d$  states allowed transition happen to final states having  $\ell$ -value as  $(0, 2)$  and  $(1, 3)$  successively. The estimated outcomes in Table VII include contributions from both  $\ell$ , for same set of  $R_a, R_b$  values of previous table. The third column collects the volume of ring ( $V = R_b^3 - R_a^3$ ) having inner and outer radii  $R_a, R_b$ . Note that,  $(R_a, R_b) = (0, 1), (0, 5), (0, 10)$  explains confined plasmas. A detailed and careful analysis of this table reveals several fascinating features, some of them are discussed below.

1. **Confined Plasmas:** In *free* plasmas,  $\alpha^{(1)}$  is a  $(+)$ ve quantity. However, in confined condition, the behavior is not so consistent, observing certain changes with  $r_c$ , presenting both  $(-)$ ve and  $(+)$ ve values. A candid conclusion appears as, with rise in  $r_c$ ,  $\alpha^{(1)}$  in a given  $n$  with an arbitrary  $\ell$  progresses as  $r_c$  approaches towards the respective *free* value. At  $r_c = 5, 10$ ,  $2s, 3s, 4s$  states possesses  $(-)$ ve polarizability.
2. **Shell-confined Plasmas:** In this environment, behavior of  $\alpha^{(1)}$  changes with  $\ell$ . For  $\ell = 0$  states, (at a given  $R_b$ ) it progresses with  $R_a$ . Similar pattern in  $\alpha^{(1)}$  is also attained by altering  $R_b$  keeping  $R_a$  fixed. Thus, it is controls by  $(R_a, R_b)$  pair, but not by their difference,  $\Delta R$ . On the contrary, for  $\ell \neq 0$  states, at a fixed  $R_b$ , it reduces with  $R_a$ . At a certain  $R_a$ , it advances with  $R_b$ . Therefore,  $\alpha^{(1)}$  is dependent on all three quantities,  $R_a, R_b, \Delta R$ .
3. **Metallic Behavior:** Through analysis of Table VII, alludes that, for  $s$ -wave states, at

TABLE VII:  $\alpha^{(1)}$  involving  $1s, 2s, 3s, 4s, 2p, 3d$  states for *confined* DP and ECSCP for  $\lambda_1, \lambda_2 = 200$

a.u.

		DP							
$R_a$	$R_b$	$V$	$\alpha_{1s}^{(1)}$	$\alpha_{2s}^{(1)}$	$\alpha_{3s}^{(1)}$	$\alpha_{4s}^{(1)}$	$\alpha_{2p}^{(1)}$	$\alpha_{3d}^{(1)}$	
0	1	1	0.02879203	0.00441401	0.00188747	0.00105362	0.01719826	0.00894345	
0.1	1	0.999	0.04759423	0.02720296	0.02357305	0.02219161	0.01004333	0.00815930	
0.2	1	0.992	0.07284697	0.05487310	0.05124971	0.04988689	0.00583027	0.00565907	
0.5	1	0.875	0.20188347	0.19133640	0.18923265	0.18848056	0.00083203	0.00083479	
0.8	1	0.488	0.43528355	0.43282925	0.43236927	0.43220785	0.00002108	0.00002108	
0.9	1	0.271	0.54241441	0.54172916	0.54160189	0.54155732	0.00000131	0.00000131	
0	5	125	3.42266613	-21.10698996	-5.69158760	-2.65406011	19.323064623	7.211907222	
0.5	5	124	19.24630056	16.11989657	15.00888999	14.25741078	6.325506169	6.027928662	
1	5	117	38.31053635	34.92820757	32.75176993	31.71721197	3.578607933	3.72435036	
2	5	109.375	90.38405129	85.34533557	83.48821755	82.73470233	1.08354091	1.09660350	
3	5	98	165.90913640	161.85818857	160.86288662	160.49302864	0.21171103	0.21200761	
4.5	5	33.875	339.00622748	338.58155053	338.50167645	338.47363010	0.00082350	0.00082314	
0	10	1000	4.49736499	-2089.73701909	-376.88040323	-143.24784214	794.443870770	171.83606073	
0.5	10	999.875	57.87595003	87.13375737	107.30929287	110.53658538	107.422952610	152.90582154	
1	10	999	163.68450247	277.64800144	254.02359344	238.62785299	80.715953070	113.77076642	
3	10	973	900.96379839	936.69782121	895.51223588	876.02414752	31.490416258	33.27278240	
5	10	875	1969.38863563	1925.74517368	1900.37617832	1889.89088703	8.272785518	8.32198498	
7.5	10	657	3873.03746168	3841.48716664	3834.24959362	3831.60721504	0.51510315	0.515184429	
9.5	10	142.625	6023.02648886	6021.22915052	6020.89380551	6020.77623107	0.00082430	0.00083429	
		ECSCP							
$R_a$	$R_b$	$V$	$\alpha_{1s}^{(1)}$	$\alpha_{2s}^{(1)}$	$\alpha_{3s}^{(1)}$	$\alpha_{4s}^{(1)}$	$\alpha_{2p}^{(1)}$	$\alpha_{3d}^{(1)}$	
0	1	1	0.02879202	0.00441401	0.00188746	0.0010536	0.01719827	0.00894345	
0.1	1	0.999	0.04759422	0.02720296	0.02357305	0.0221916	0.01004333	0.00815930	
0.2	1	0.992	0.07284696	0.05487311	0.05124971	0.0498868	0.00583027	0.00565907	
0.5	1	0.875	0.20188347	0.19133640	0.18923265	0.1884805	0.00083203	0.00083479	
0.8	1	0.488	0.43528355	0.43282925	0.43236927	0.432207	0.00002108	0.00002108	
0.9	1	0.271	0.54241441	0.54172916	0.54160189	0.541557	0.00000131	0.00000131	
0	5	125	3.42245701	-21.10658875	-5.69164013	-2.654078177	18.089256906	7.211969349	
0.5	5	124	19.24560240	16.12002214	15.00896003	14.25745461	6.325398881	6.027953552	
1	5	117	38.30978377	34.92836926	32.75186619	31.7172717	3.578571649	3.724345497	
2	5	109.375	90.38359628	85.34545140	83.48828806	82.7347460	1.08353814	1.096601690	
3	5	98	165.90899543	161.85822837	160.86291039	160.4930432	0.21171096	0.21200753	
4.5	5	33.875	339.00622801	338.58155153	338.50167840	338.4736317	0.00082310	0.00082305	
0	10	1000	4.49682336	-2086.57335851	-376.86974059	-143.2486061	793.3606562289	171.83710421	
0.5	10	999.875	57.86098336	87.17797675	107.31666530	110.540461660	107.386951511	152.90392715	
1	10	999	163.64384127	277.67453375	254.03439794	238.63393904	80.695671484	113.766036855	
3	10	973	900.89151483	936.71840975	895.52388818	876.03124518	31.488571915	33.27162531	
5	10	875	1969.35464432	1925.75459775	1900.38182210	1889.89436868	8.27270253	8.321916505	
7.5	10	657	3873.03398162	3841.48819175	3834.25021073	3831.6076104	0.51510319	0.515184124	
9.5	10	142.625	6023.02653188	6021.22924375	6020.89380928	6020.7762564	0.00080937	0.0008319	

TABLE VIII: Calculated  $R_a = R_m$  at ten  $R_b$ , involving  $1s, 2s, 3s, 4s$  states in *shell-confined* DP and ECSCP ( $\lambda_1, \lambda_2 = 200$  a.u) in field free condition.

$R_a = R_m$								
$R_b$	DP				ECSCP			
	1s	2s	3s	4s	1s	2s	3s	4s
1	0.81776350	0.81844600	0.81857200	0.81861640	0.81776351	0.81844574	0.81857220	0.81861648
2	1.38054800	1.38696390	1.38819670	1.38863160	1.38054798	1.38696390	1.38819666	1.38863163
3	1.78705437	1.80680400	1.81094670	1.81243570	1.78705451	1.80680395	1.81094673	1.81243570
4	2.09184539	2.13011530	2.13937730	2.14279860	2.09184635	2.13011505	2.13937718	2.14279852
5	2.32953256	2.38598612	2.40275121	2.40915329	2.32953642	2.38598518	2.40275066	2.40915295
6	2.52409956	2.59179190	2.61850445	2.62907944	2.52411065	2.59178916	2.61850286	2.62907847
7	2.69276190	2.75851277	2.79764248	2.81370398	2.69278753	2.75850619	2.79763871	2.81370171
8	2.84777754	2.89338024	2.94745556	2.97042156	2.84782806	2.89336637	2.94744777	2.97041687
9	2.99755944	3.00126635	3.07296888	3.10435211	2.99764801	3.00123984	3.07295433	3.10434343
10	3.14757096	3.08545126	3.17775868	3.21916532	3.14771290	3.08540435	3.17773352	3.21915040

a certain  $R_b$ ,  $\alpha^{(1)}$  progresses with  $R_a$ . But, for  $2p, 3d$  states reverse trend is observed. Moreover, for  $\ell = 0$  states there appears a characteristic  $R_a$  after which it prevails over  $V$ . Now, invoking the *Herzfeld* criteria for *insulator to metal* conversion discussed in Eq. (14)-(16), one may easily discern the metallic character for  $s$ -wave states in *shell-confined* hydrogenic plasmas (both DP and ECSCP). It should be kept in mind that, no such feature is observed for  $\ell \neq 0$  states. The threshold  $R_a$  at which Eq. (16) is obeyed or  $\alpha^{(1)}$  becomes equal to  $V$  is symbolized as  $R_m$ . They are reported in Table VIII, for  $\ell = 0$  states at ten selected  $R_b$  values (1, 2, 3, 4, 5, 6, 7, 8, 9, 10). In either of the plasmas, the the spread of the metallic region ( $R_b - R_a$ ) increases with progress in  $R_b$ .

Tables VII and VIII assert the existence of metallic character in *shell-confined* DP and ECSCP. But, they are not able to ascertain the similar behavior in when  $R_a = 0$ ; i.e. in confined condition. Therefore, we have investigated  $\alpha^{(1)}$  as a function of  $\lambda$  in these two confined plasmas, keeping  $r_c$  fixed at some arbitrary chosen values. It is useful to point out that, in relevant figures metallic ( $\alpha^{(1)} > V$ ) and non-metallic ( $\alpha^{(1)} < V$ ) regions are mentioned with *green* and *red* colors. Further,  $\alpha^{(1)} = V$  is represented by a black straight line.

Figure 1 imprints the behavior  $\alpha^{(1)}$  for ground state in DP with change in  $\lambda_1$  opting  $r_c$  fixed at four selected values, namely 1, 5, 10, 20. In all these cases it progresses with growth

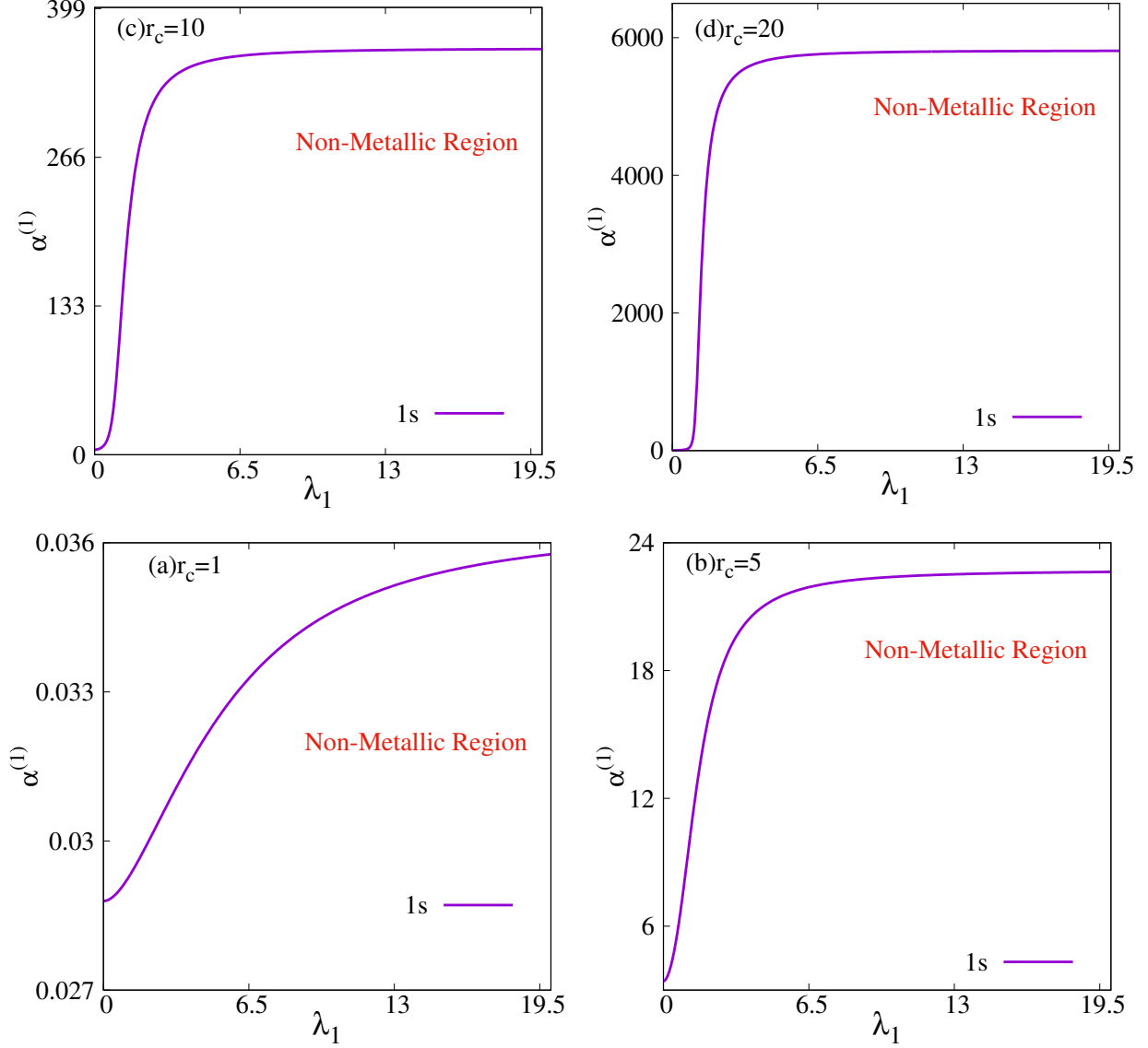


FIG. 1:  $\alpha^{(1)}$  values for 1s state in DP as a function of  $\lambda_1$  at  $r_c$  values 1, 5, 10, 20.

in  $\lambda_1$ . More importantly,  $\alpha^{(1)} < V$ , condition is obeyed. Therefore, metallic character is not seen. However, for higher states with  $\ell = 0$ , reverse pattern is seen. These has been discussed in Figure 2 and 3 involving 2s, 3s states.

Figure 2 depicts the behavior  $\alpha^{(1)}$  for 2s state in DP with progress in  $\lambda_1$  keeping  $r_c$  fixed at four selected values, namely 10, 15, 20, 40. In panels (a) ( $r_c = 10$ ) and (d) ( $r_c = 40$ ),  $\alpha^{(1)} < V$ . On the contrary, at panels (b) ( $r_c = 15$ ) and (c) ( $r_c = 20$ ) there exists a range of  $\lambda_1$ , where  $\alpha^{(1)} > V$ . It suggests, that for 2s state there appears a region of  $\lambda_1, r_c$ , at which metallic pattern is observed.

Figure 3 portrays the behavior  $\alpha^{(1)}$  for 3s state in DP with growth in  $\lambda_1$  keeping  $r_c$  fixed



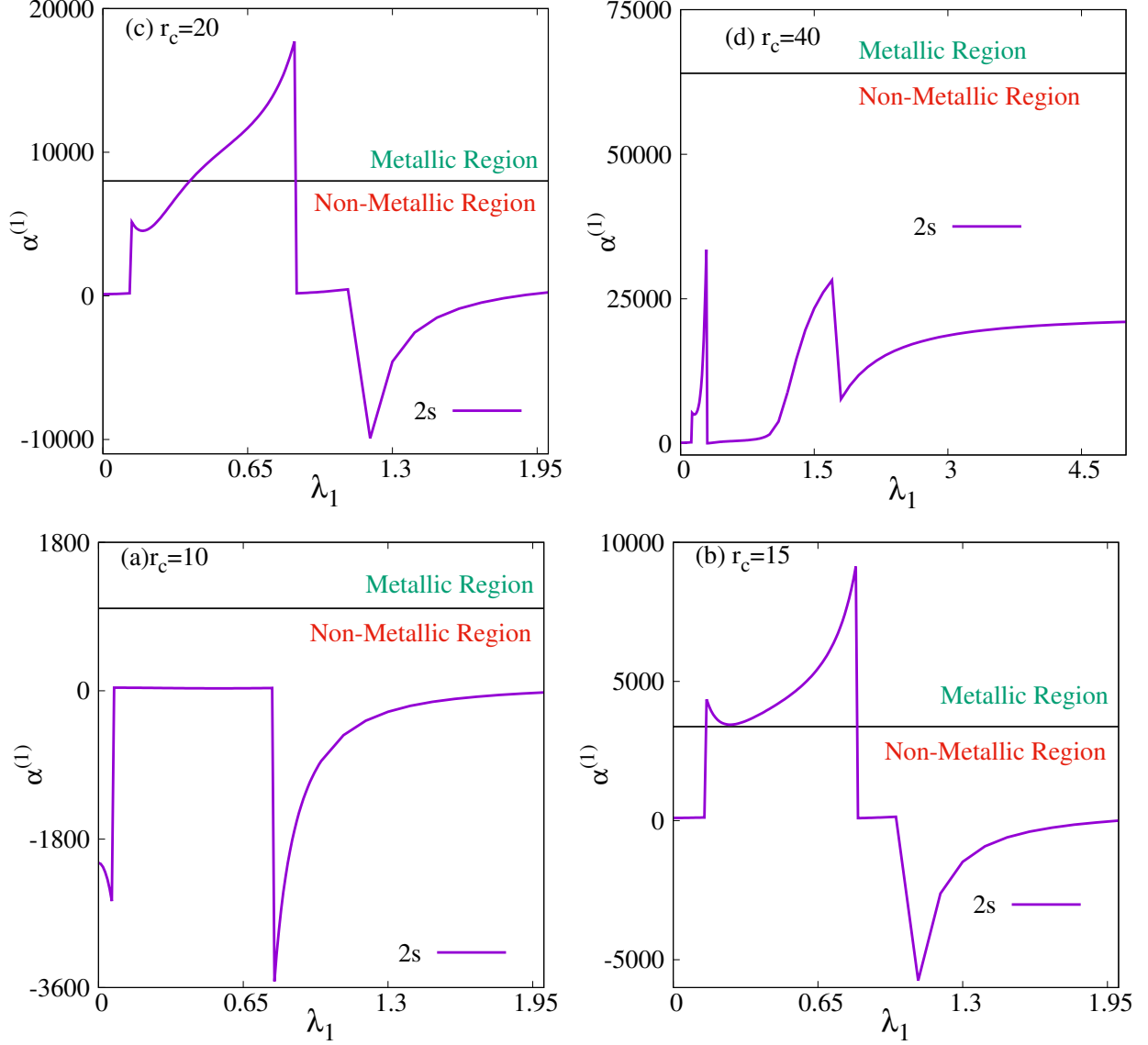


FIG. 2:  $\alpha^{(1)}$  values for  $2s$  state in DP as a function of  $\lambda_1$  at  $r_c$  values 10, 15, 20, 40.

at four selected values, namely 15, 20, 30, 50. Similar to Fig. 2, in panels (a) ( $r_c = 15$ ) and (d) ( $r_c = 50$ ) metallic nature is not observed. However, at panels (b) ( $r_c = 15$ ) and (c) ( $r_c = 20$ ) there appears a range of  $\lambda_1$ , where  $\alpha^{(1)} > V$ . Akin to  $2s$  state, it indicates the presence of metallic like behavior in  $3s$  at a certain range of  $\lambda_1$ . Resembling nature is seen ECSCP. In  $1s$  state,  $\alpha^{(1)} < V$ . But, in  $2s, 3s$  there exists a range of  $r_c$  and  $\lambda_2$  at which  $\alpha^{(1)} > V$ . These, are demonstrated in Figs. S1-S3 for  $1s, 2s, 3s$  states respectively in supporting document.

TABLE IX:  $f^{(1)}$  involving  $1s, 2s, 2p$  states for *confined* DP and ECSCP for  $\lambda_1, \lambda_2 = 200$  a.u under external electric field ( $\cos \theta = 1$  and  $F=0.1$  a.u.).

		DP							
$R_a$	$R_b$	$1s \rightarrow 2p$	$1s \rightarrow 3p$	$2s \rightarrow 2p$	$2s \rightarrow 3p$	$2p \rightarrow 1s$	$2p \rightarrow 2s$	$2p \rightarrow 3d$	$2p \rightarrow 4d$
0	1	0.9847251914	0.0075938816	-0.6085532464	1.5607501708	-0.3282417304	0.2028510821	1.084947173	0.018477266
0.1	1	0.8992558694	0.0910315700	-0.5489683137	1.2678876762	-0.2997519564	0.1829894379	1.078377462	0.025699465
0.2	1	0.8116440851	0.1765877949	-0.4644217903	1.0122462837	-0.2705480283	0.1548072634	1.044551812	0.059606046
0.5	1	0.6974624555	0.2896426262	-0.3508436517	0.7344809882	-0.2324874851	0.1169478839	0.929552195	0.173158739
0.8	1	0.6699145823	0.3169995731	-0.3234507104	0.6737046143	-0.2233048607	0.1078169034	0.893218987	0.209183950
0	5	0.8361380309	0.1187719538	-0.4652011227	1.4311008380	-0.2787126769	0.1550670409	1.105185469	0.000589816
0.5	5	0.9366780393	0.0448308778	-0.5889293266	1.3448509199	-0.3122260131	0.1963097755	1.104946243	0.002554739
1	5	0.8237623348	0.1582743437	-0.4739946689	1.0327399751	-0.2745874449	0.1579982229	1.061528816	0.043156235
2	5	0.7205324739	0.2657408559	-0.3731447891	0.7862129590	-0.2401774913	0.1243815963	0.958949133	0.143774708
3	5	0.6836004488	0.3033256461	-0.3369872946	0.7036150442	-0.2278668162	0.1123290982	0.911407603	0.191100634
4.5	5	0.6673917783	0.3195048401	-0.3209450002	0.6682356569	-0.2224639261	0.1069816667	0.889855694	0.212523222
0	10	0.7350528262	0.1273164444	-0.3851990415	1.1787776832	-0.2450176087	0.1283996805	1.046533203	0.049105808
0.5	10	0.9670417912	0.0012262145	-0.5679581943	1.5172373747	-0.3223472637	0.1893193981	1.077766994	0.028556724
1	10	0.8889278408	0.0487087750	-0.4646558626	1.2615685051	-0.2963092802	0.1548852875	1.102614229	0.000860195
3	10	0.7466750512	0.2020146050	-0.3576526692	0.8573304191	-0.2488916837	0.1192175564	0.994558887	0.089926534
5	10	0.6973476916	0.2823588053	-0.3433822012	0.7345308100	-0.2324492305	0.1144607337	0.929687318	0.168722142
7.5	10	0.6720674882	0.3147416988	-0.3254733528	0.6783789204	-0.2240224960	0.1084911176	0.896088365	0.206260559
9.5	10	0.6668385720	0.3200542481	-0.3203956762	0.6670385229	-0.2222795240	0.1067985587	0.889118103	0.213255692
		ECSCP							
$R_a$	$R_b$	$1s \rightarrow 2p$	$1s \rightarrow 3p$	$2s \rightarrow 2p$	$2s \rightarrow 3p$	$2p \rightarrow 1s$	$2p \rightarrow 2s$	$2p \rightarrow 3d$	$2p \rightarrow 4d$
0	1	0.984725212	0.0075938865	-0.608553283	1.560750223	-0.328241737	0.202851094	1.0849471891	0.0184772537
0.1	1	0.899255888	0.091031551	-0.548968340	1.267887712	-0.299751962	0.182989446	1.0783774765	0.0256994536
0.2	1	0.811644092	0.176587787	-0.464421799	1.012246295	-0.270548030	0.154807266	1.0445518211	0.0596060389
0.5	1	0.697462455	0.289642626	-0.350843651	0.734480988	-0.232487485	0.116947883	0.9295521960	0.1731587395
0.8	1	0.669914582	0.316999573	-0.323450710	0.673704615	-0.223304860	0.107816903	0.8932189877	0.2091839509
0	5	0.836137691	0.118772104	-0.465203014	1.431102312	-0.278712563	0.155067671	1.1051853164	0.0005901275
0.5	5	0.936678057	0.044830133	-0.588928807	1.344851790	-0.312226019	0.196309602	1.1049468363	0.0025542979
1	5	0.823762447	0.158273646	-0.473994298	1.032740340	-0.274587482	0.157998099	1.0615293802	0.0431556044
2	5	0.720532508	0.265740711	-0.373144730	0.786213020	-0.240177502	0.124381576	0.9589492016	0.1437745964
3	5	0.683600451	0.303325634	-0.336987289	0.703615049	-0.227866817	0.112329096	0.9114076082	0.1911006258
4.5	5	0.667391775	0.319504839	-0.320945000	0.668235652	-0.222463925	0.106981666	0.8898556952	0.2125232225
0	10	0.7350652410	0.127312341	-0.385213057	1.178794763	-0.245021747	0.128404352	1.0465359219	0.0491034056
0.5	10	0.9670396465	0.001226961	-0.567954594	1.517230060	-0.322346548	0.189318198	1.0777697522	0.0285543193
1	10	0.8889230773	0.048712046	-0.464649283	1.261557925	-0.296307692	0.154883094	1.1026139362	0.0008596678
3	10	0.7466728691	0.202012739	-0.357645614	0.857327035	-0.248890956	0.119215204	0.9945564080	0.0899265442
5	10	0.6973475211	0.282357651	-0.343380662	0.734530589	-0.232449173	0.114460220	0.9296871195	0.1687215263
7.5	10	0.6720674892	0.314741675	-0.325473330	0.678378921	-0.224022496	0.108491110	0.8960883658	0.2062605435
9.5	10	0.6668385642	0.320054248	-0.320395676	0.667038519	-0.222279521	0.106798558	0.8891181123	0.2132556921

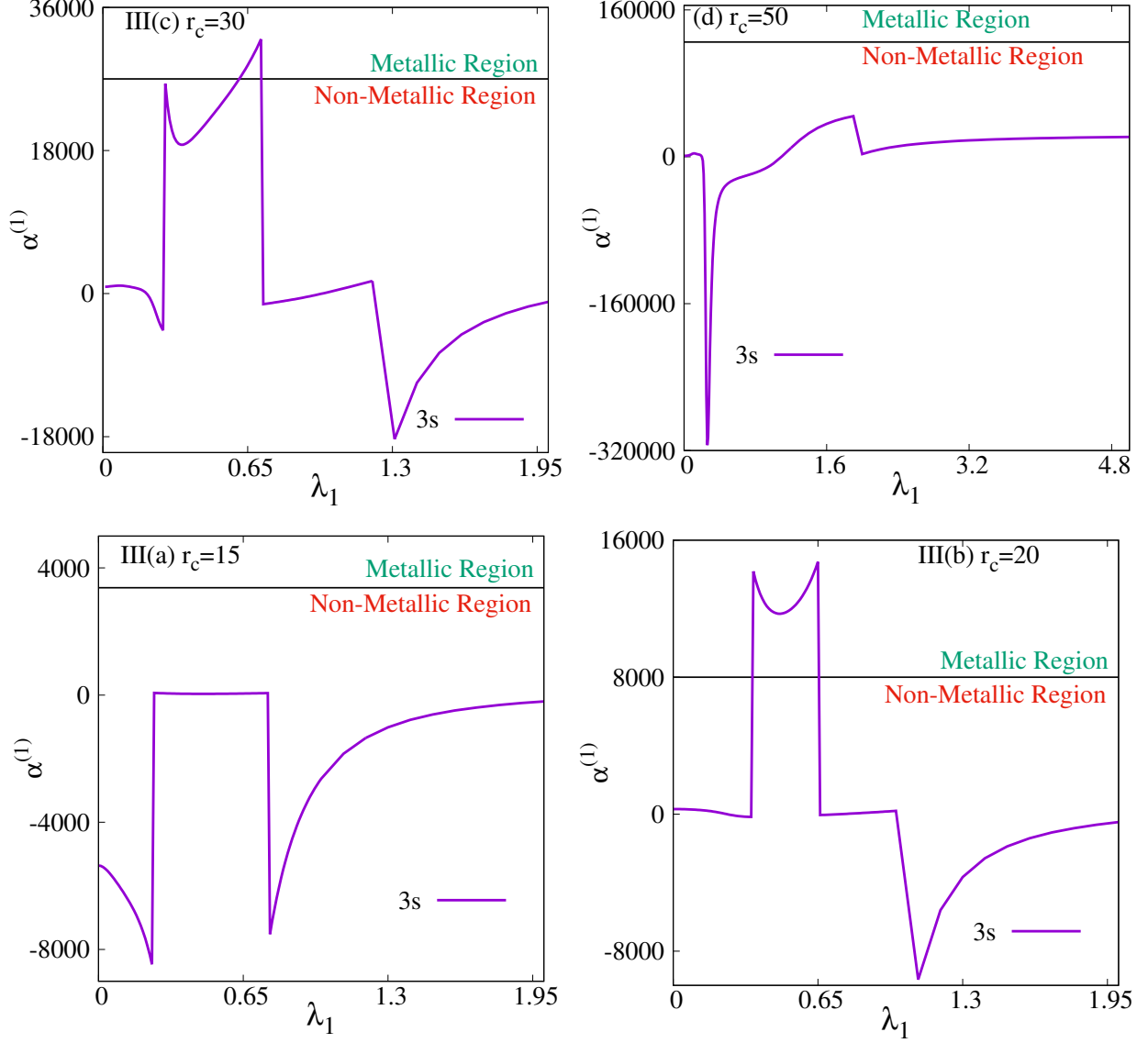


FIG. 3:  $\alpha^{(1)}$  values for 3s state in DP as a function of  $\lambda_1$  at some selected  $r_c$  values. See text for details.

### C. Influence of External Electric field

In this section we discuss about the effect of external electric field on  $f^{(1)}$  and  $\alpha^{(1)}$ . For obvious reason the numerical value will change. Here, we aim to discuss the change in their quantitative and qualitative pattern.

Table IX presents estimated  $f^{(1)}$  for 1s, 2s, 2p states connecting  $n, \ell \rightarrow n', (\ell + 1)$  transitions ( $n = 1, 2; n' = 2, 3, 4$ ) relating DP and ECSCP. Alike the field free situation, in either of the plasmas, SCC outcomes are reported for three  $R_b$ , namely, 1, 5, 10; for each  $R_b$ ,  $R_a$  alters from  $0 - R_b$ . Here, CS situation is attained when  $R_a = 0$  and  $r_c = R_b = 1, 5, 10$ .

Now, Comparing the results in Tables VI and IX for both DP and ECSCP, it is found that, for all possible transitions the qualitative pattern of  $f^{(1)}$  (with increase in  $R_a$  at a certain  $R_b$ ) in  $F = 0$  and  $F = 0.1$  a.u. are similar. Further, analysis also discloses that, in some  $R_a, R_b$ , the  $f^{(1)}$  values in electric field are higher to respective field free cases. However, this behavior gets reversed in other sets of  $R_a, R_b$  values.

Table X, represents the  $\alpha^{(1)}$  values at  $F = 0.1$  a.u. involving  $1s, 2s, 2p, 3s, 3d, 4s$  states using same set of  $R_a, R_b$  values of Table VII. In-depth comparison of Tables VII and X for both DP and ECSCP reveals several interesting features, some of them are discussed below.

1. For  $1s, 2p, 3d$  states,  $\alpha^{(1)}$  in presence of external field possesses higher value compare to its free counterpart. However, for  $2s, 3s, 4s$  states behavior is not very consistent.
2. Similar to field free cases, here also  $\alpha^{(1)}$  can have both  $-ve$  and  $+ve$  values. Particularly, for  $2s, 3s, 4s$  state such phenomena is observed.
3. For  $1s, 2s, 3s, 4s$  states metallic behavior is observed after a threshold value of  $R_a$  (at a fixed  $R_b$ ).
4. The threshold  $R_a$  at which Eq. (16) is valid are reported in Table S1 in supporting document, for  $1s, 2s, 3s, 4s$  states at ten selected  $R_b$  values (1, 2, 3, 4, 5, 6, 7, 8, 9, 10). As usual, in either of the plasmas, the spread of the metallic region ( $R_b - R_a$ ) increases with growth in  $R_b$ .

Now, to move to investigate the effect of field strength  $F \cos \theta$  on  $\alpha^{(1)}$ . In this context, pilot calculations are done at six separate sets of  $(\lambda, r_c)$ , they are (0, 5), (0, 10), (0.25, 5), (0.25, 10), (0.5, 5), (0.5, 10). Panels (a)-(b) in Fig. 4, imprints the change in  $\alpha^{(1)}$  values with advancement of  $F \cos \theta$  in  $1s$  state of DP at three different  $\lambda_1$  values keeping  $r_c$  fixed at 5 and 10 respectively. At a certain  $\lambda_1, r_c$  it decreases with increase in field strength. However, at a fixed  $r_c$ , it increases with increase in  $\lambda_1$ . Following the same line,  $\alpha^{(1)}$  in  $2s$  state is plotted in panels (c)-(d) in Fig. (4) at the same six sets of  $\lambda, r_c$ . It is interesting to point out that,  $\alpha^{(1)}$  behaves differently with at  $r_c = 5$  and 10 successively. At  $r_c = 5$  (panel (c)),  $\alpha^{(1)}$  increases with progress in  $F \cos \theta$ . Further, it possesses  $-ve$  value through the range of field strength. Panel (d) ( $r_c = 10$ ), shows that, at  $\lambda_1 = 0$ , starting from initial  $-ve$  value it increases with rise in  $F \cos \theta$ . However, at  $\lambda_1 = 0.25, 0.50$ , it has

TABLE X:  $\alpha^{(1)}$  involving  $1s, 2s, 3s, 4s, 2p, 3d$  states for *confined* DP and ECSCP for  $\lambda_1, \lambda_2 = 200$  a.u under external electric field ( $\cos \theta = 1$  and  $F=0.1$  a.u.).

		DP						
$R_a$	$R_b$	$V$	$\alpha_{1s}^{(1)}$	$\alpha_{2s}^{(1)}$	$\alpha_{3s}^{(1)}$	$\alpha_{4s}^{(1)}$	$\alpha_{2p}^{(1)}$	$\alpha_{3d}^{(1)}$
0	1	1	0.028685	0.004388	0.001881	0.001051	0.017199	0.008949
0.1	1	0.999	0.047490	0.027205	0.023578	0.022195	0.010040	0.008163
0.2	1	0.992	0.072756	0.054885	0.051259	0.049892	0.005828	0.005659
0.5	1	0.875	0.201853	0.191344	0.189237	0.188483	0.000831	0.000834
0.8	1	0.488	0.435282	0.432829	0.432369	0.432208	0.000021	0.000021
0.9	1	0.271	0.542414	0.541729	0.541601	0.541557	0.000001	0.000001
0	5	125	2.226123	-16.206022	-6.075753	-2.798394	14.243414	7.531339
0.5	5	124	14.491464	17.233694	15.605856	14.624534	5.339967	6.074421
1	5	117	32.680314	36.281979	33.559364	32.214396	3.235514	3.620504
2	5	109.375	86.698183	86.313674	84.075106	83.097143	1.057095	1.077750
3	5	98	164.739292	162.187970	161.061777	160.615365	0.210925	0.211306
4.5	5	33.875	338.998393	338.583878	338.503064	338.474480	0.000823	0.000822
0	10	1000	2.366994	-48.314349	-136.574119	-139.154836	36.960919	54.924054
0.5	10	999.875	19.832366	96.855198	161.913457	147.664876	16.315774	46.140319
1	10	999	54.975240	231.979757	331.570336	295.289062	14.768745	32.917260
3	10	973	519.371381	1021.276070	997.344383	938.787431	14.713720	17.336989
5	10	875	1704.365561	2003.187148	1949.618672	1920.054765	7.088535	7.230665
7.5	10	657	3842.733924	3850.397128	3839.576947	3834.873737	0.512541	0.512695
9.5	10	142.625	6022.958766	6021.249474	6020.905887	6020.783761	0.000805	0.000827
		ECSCP						
$R_a$	$R_b$	$V$	$\alpha_{1s}^{(1)}$	$\alpha_{2s}^{(1)}$	$\alpha_{3s}^{(1)}$	$\alpha_{4s}^{(1)}$	$\alpha_{2p}^{(1)}$	$\alpha_{3d}^{(1)}$
0	1	1	0.028685	0.004388	0.001881	0.001051	0.017199	0.008949
0.1	1	0.999	0.047490	0.027205	0.023578	0.022195	0.010040	0.008163
0.2	1	0.992	0.072756	0.054885	0.051259	0.049892	0.005828	0.005659
0.5	1	0.875	0.201853	0.191344	0.189237	0.188483	0.000831	0.000834
0.8	1	0.488	0.435282	0.432829	0.432369	0.432208	0.000021	0.000021
0.9	1	0.271	0.542414	0.541729	0.541601	0.541557	0.000001	0.000001
0	5	125	2.226022	-16.205347	-6.075795	-2.798411	14.242942	7.531355
0.5	5	124	14.490991	17.233831	15.605931	14.624579	5.339841	6.074408
1	5	117	32.679698	36.282142	33.559464	32.214457	3.235469	3.620484
2	5	109.375	86.697749	86.313791	84.075178	83.097187	1.057092	1.077747
3	5	98	164.739152	162.188009	161.061801	160.615380	0.210925	0.211306
4.5	5	33.875	338.998394	338.583881	338.503067	338.474481	0.000823	0.000822
0	10	1000	2.366863	-48.305017	-136.552211	-139.150610	36.955529	54.916435
0.5	10	999.875	19.830950	96.847711	161.914596	147.669598	16.313636	46.133709
1	10	999	54.971399	231.964474	331.573761	295.296156	14.766828	32.912464
3	10	973	519.346824	1021.271740	997.355997	938.795020	14.712319	17.335371
5	10	875	1704.338447	2003.194993	1949.624430	1920.058295	7.088361	7.230499
7.5	10	657	3842.730471	3850.398145	3839.577555	3834.874125	0.512541	0.512695
9.5	10	142.625	6022.958829	6021.249507	6020.906043	6020.783663	0.000762	0.000842

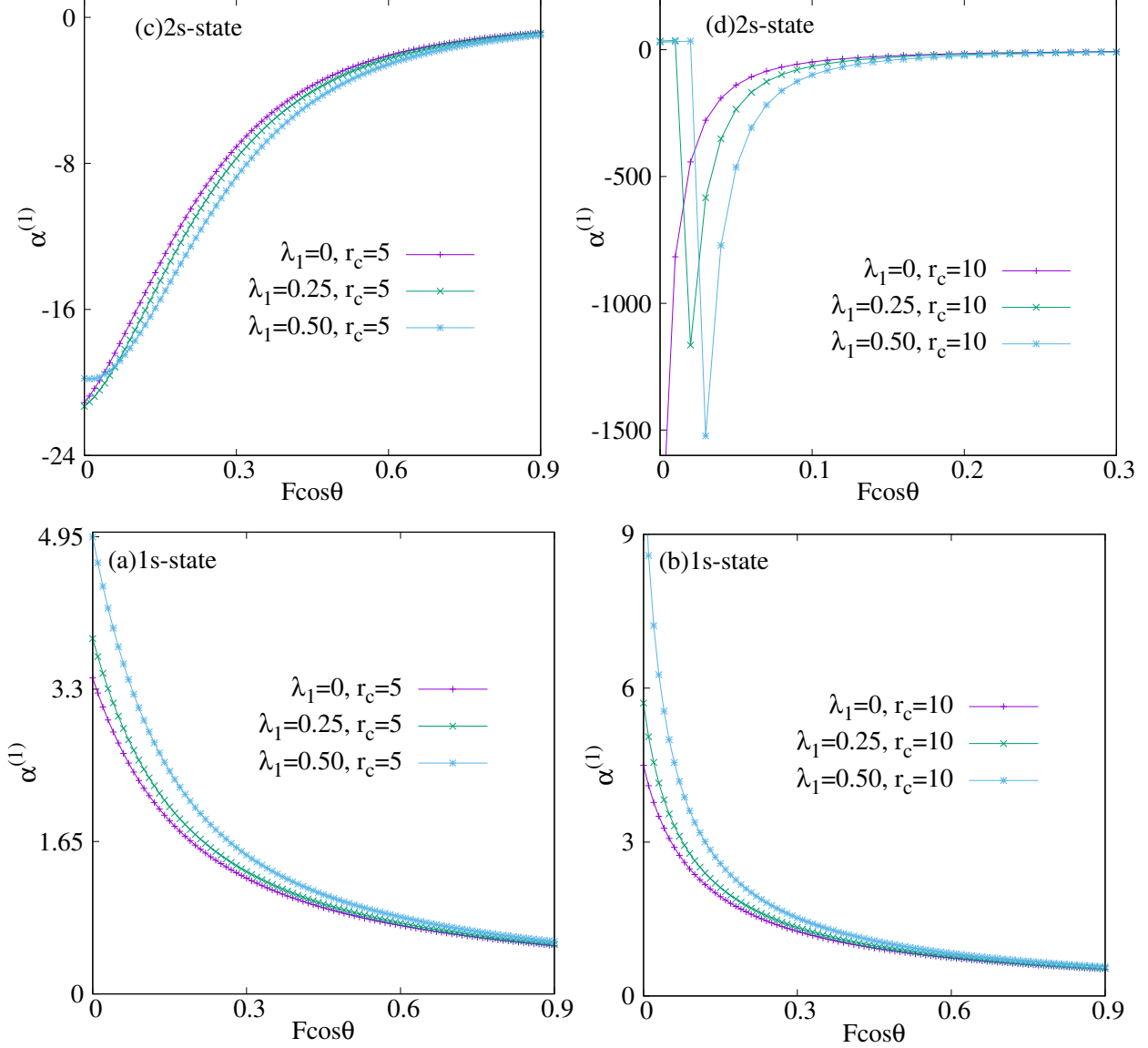


FIG. 4:  $\alpha^{(1)}$  values for  $1s, 2s$  states in DP as a function of  $F \cos \theta$  at some selected  $\lambda_1$  values.

+ve value at the beginning. Then sharply reduces to -ve value. Finally, after reaching the minimum it increases but never becomes -ve.

Figure 5, reveals the behavior of  $\alpha^{(1)}$  in ECSCP with increase in field strength. Panels (a)-(b) portrays the outcome for  $1s$  state at same six sets of  $\lambda, r_c$  values. The ground state of ECSCP exhibit exactly similar pattern to DP with obvious changes in their numerical values. Moreover, in  $2s$  state at  $r_c = 5$  (panel (c)) we observe identical nature. But, at  $r_c = 10$  (panels (d)) distinguished shift is observed at  $\lambda_2 = 0.25, 0.50$ . In these cases, with rise in field strength,  $\alpha^{(1)}$  sharply drops closes to *zero* to reach a flat plateau then again exquisitely falls to a minimum and finally increases.

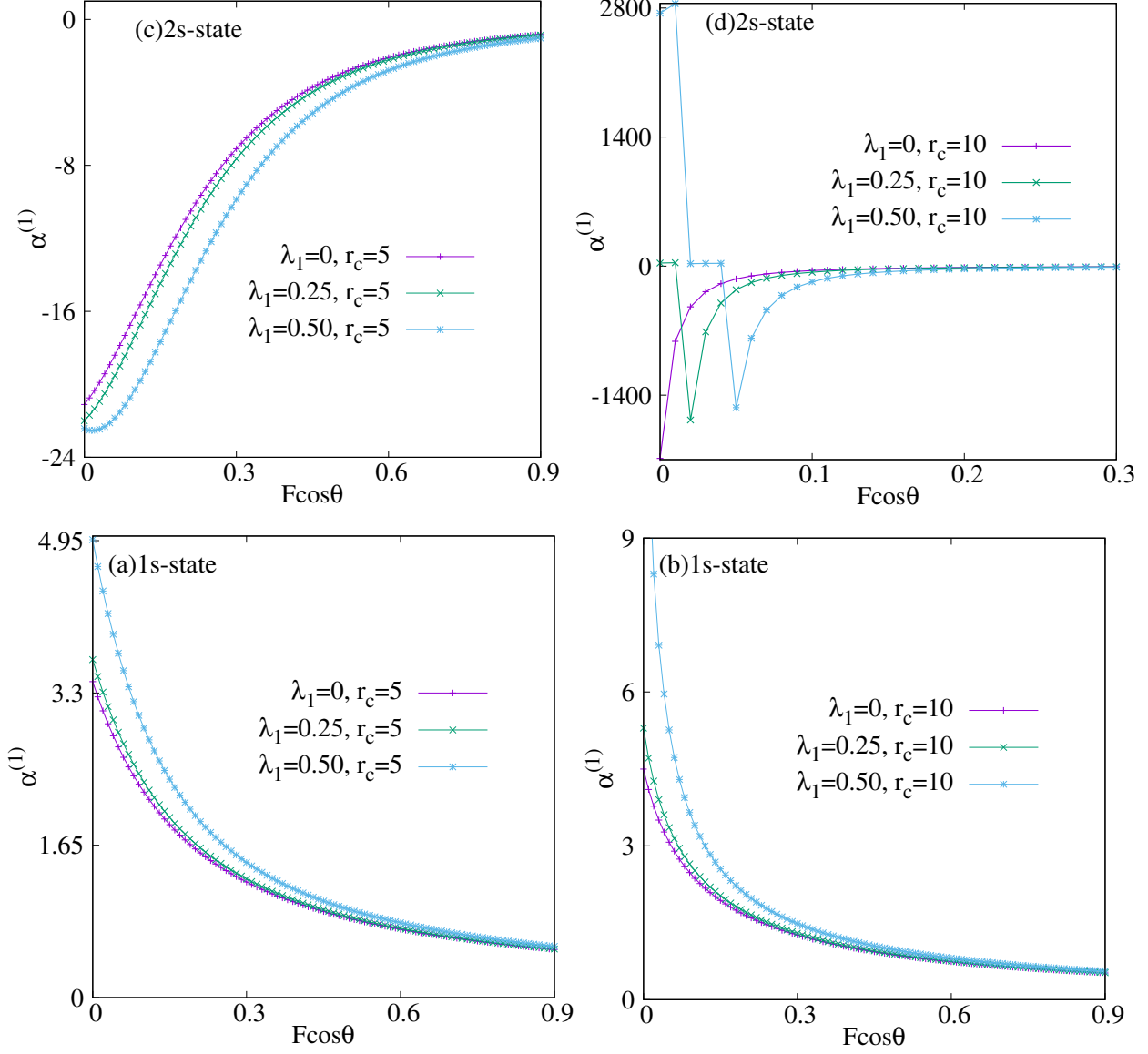


FIG. 5:  $\alpha^{(1)}$  involving  $1s, 2s$  states in ECSCP as a function of  $F \cos \theta$  at some selected  $\lambda_2$  values.

Now, we probe the influence of  $\lambda$  on the metallic behavior of *shell-confined* DP and ECSCP in  $F \cos \theta = 0$  and  $F \cos \theta = 0.1$  a.u. at two different  $R_b$  namely, 5, 10 in  $1s, 2s$  states. Here,  $R_a$  has been opted as the respective  $R_m$  values. The bottom panels (a)-(b) of Fig. 6 demonstrates the results in  $1s$  state for  $r_c = 5, 10$  respectively under field free conditions. In both DP and ECSCP  $\alpha^{(1)} > V$  through out the range of  $\lambda$ . For both  $R_b$ ,  $\alpha^{(1)}$  increases with increase in  $\lambda_1$ . However, in ECSCP, in either of  $R_b$ , it advances to a maximum then approaches to respective DP limits. Further, the top panels (c)-(d) exhibit the same for  $F \cos \theta = 0.1$  a.u. In this case identical behavioral pattern to field free condition is observed for both DP and ECSCP. In essence, it can be said that, in both the plasmas

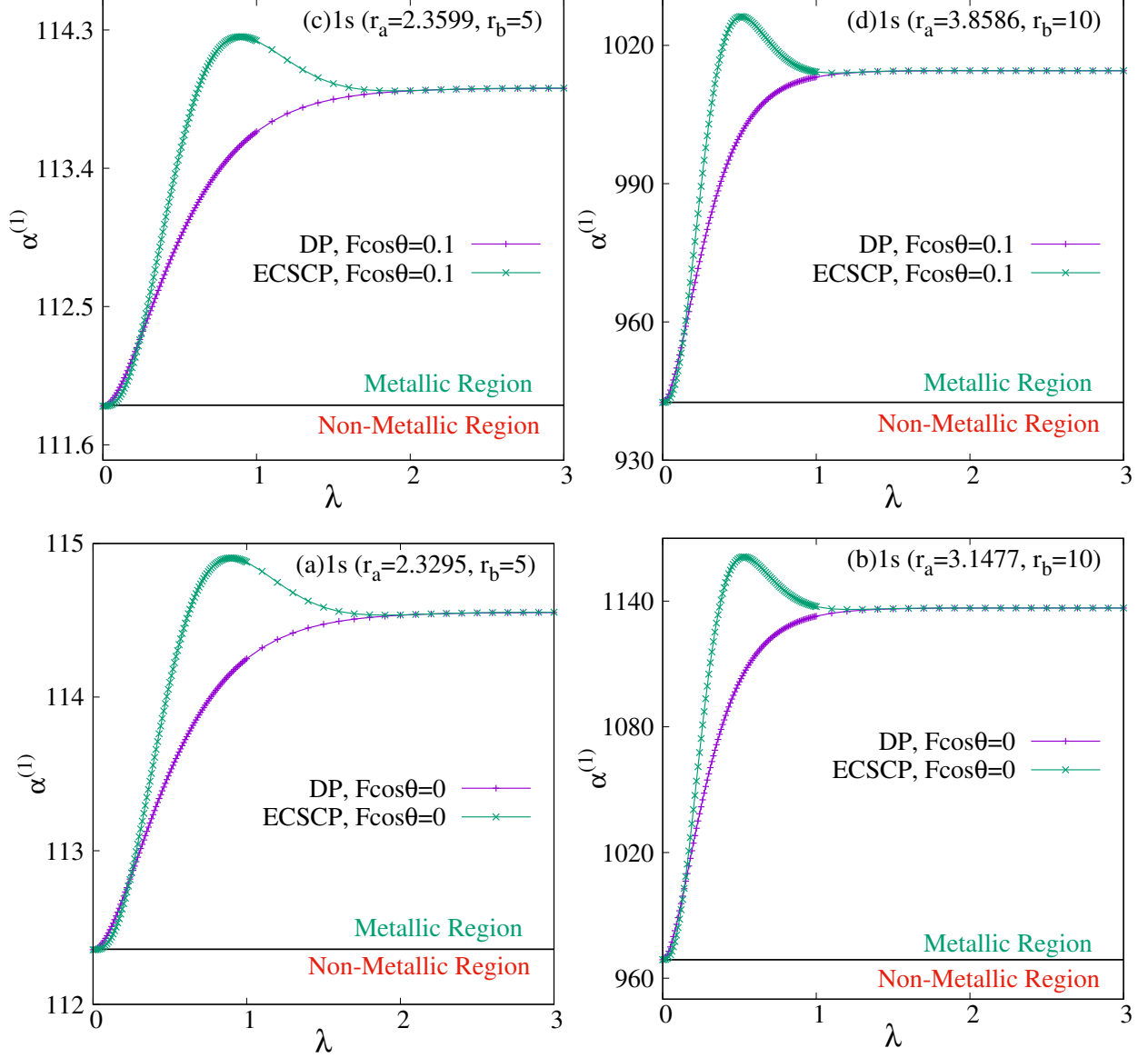


FIG. 6:  $\alpha^{(1)}$  values for  $1s$  state in DP, ECSCP as a function of  $\lambda$  at two different  $r_b$  (5, 10 a.u.) values choosing  $F \cos \theta = 0$  and  $F \cos \theta = 0.1 a.u.$ .

metallic character in ground state increases with increase in  $\lambda$ .

The panels (a)-(c) in Fig. 7 explains the change in  $\alpha^{(1)}$  with rise in  $\lambda$  in  $2s$  state of *shell-confined* DP and ECSCP at  $R_b = 5$  involving  $F \cos \theta = 0$ ,  $F \cos \theta = 0.1$  a.u. successively. It is necessary to mention that, at the onset  $\alpha^{(1)} > V$ , but with rise in  $\lambda$ , we observe reverse scenario ( $\alpha^{(1)} < V$ ). In DP involving both  $F \cos \theta = 0$ ,  $F \cos \theta = 0.1$  a.u. cases,  $\alpha^{(1)}$  decreases with rise in  $\lambda_1$ . However, in ECSCP in either of the conditions, it decreases to reach a minimum then increases to attain a shallow maximum before merging to respective DP values. Panel (c)-(d) indicate the changes of  $\alpha^{(1)}$  with and with out field respectively at



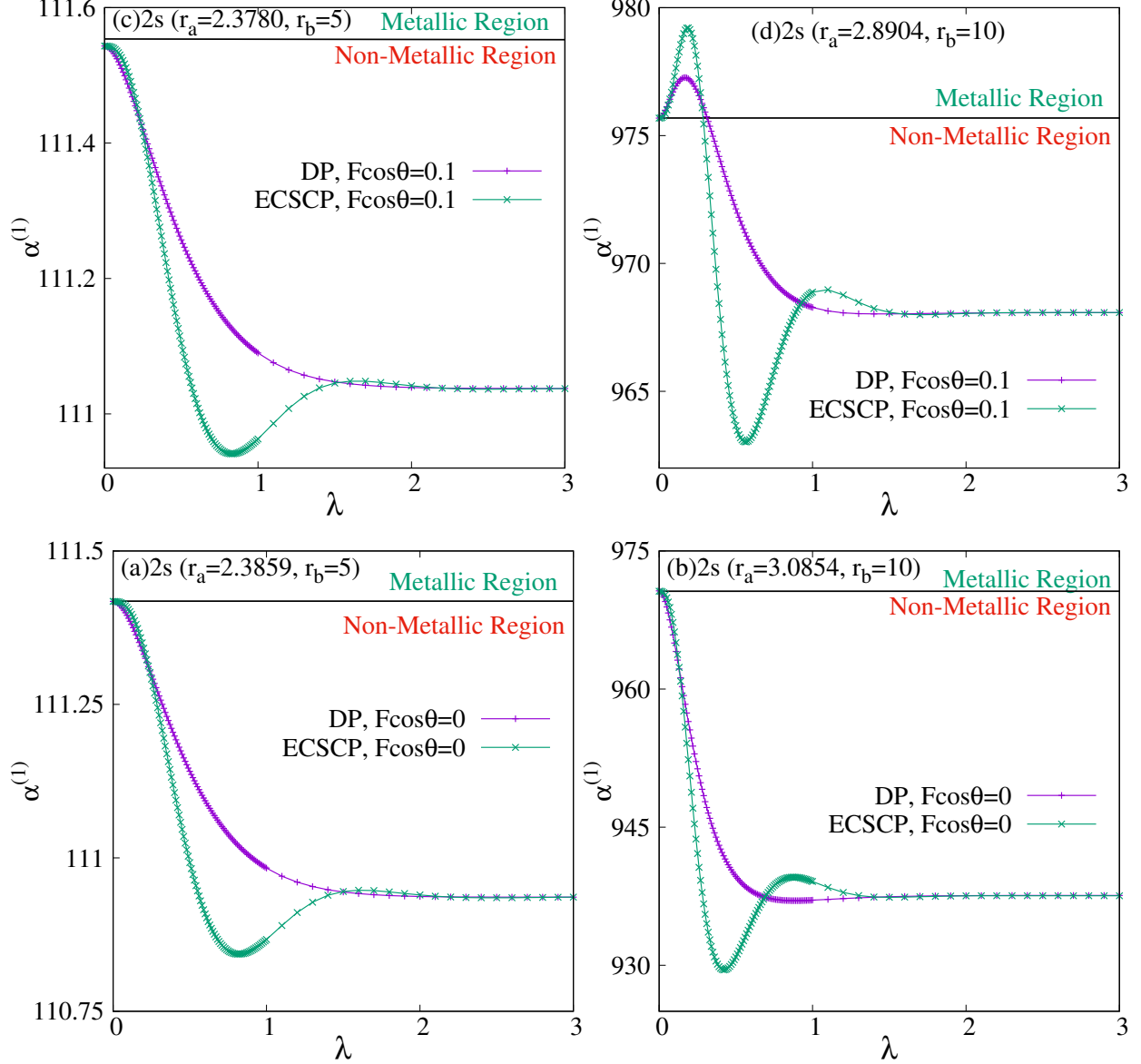


FIG. 7:  $\alpha^{(1)}$  values for  $2s$  state in DP, ECSCP as a function of  $\lambda$  at two different  $r_b$  (5, 10 a.u) values choosing  $F \cos \theta = 0$  and  $F \cos \theta = 0.1 a.u.$ .

$R_b = 10$ . As usual the initial  $\alpha^{(1)}$  values are higher than  $V$ . In field free DP, it decreases with progress in  $\lambda_1$ . However, under the external electric field it increase to reach a maximum then reduces. In ECSCP, relating filed free case, it decreases to approach a minimum then increases to a prominent maximum before reaching to DP values. At  $F \cos \theta = 0.1$  a.u, it climbs a maximum then falls down to a minimum and again attains a maximum to convene to DP limit.

## V. FUTURE AND OUTLOOK

Degeneracies, dipole oscillator strength and polarizability have been investigated for confined DP and ECSCP applying GCS model with special emphasis on *shell-confined* condition, which has not been done before. This model can illustrate both *confined* and *free* conditions efficiently. Effect of external electric field on these properties is also elaborately investigated. Impact of field strength on these spectroscopic properties is also probed. An in-depth analysis reveals several impressive and hitherto unreported characteristics in these plasmas. Existence of an additional degeneracy in weakly coupled plasmas under confined environment has also been established. In GCS with growth in  $n$ , count of these incidental degenerate states increases, conversely, at a fixed  $n$ , with rise in  $\ell$ , their number decreases. In stressed condition, *negative* polarizability is experienced in excited states. Further, metallic nature is observed in both *confined* and *shell-confined* conditions. The influence of  $R_a, R_b$  on spectroscopic properties are probed. Similar calculations in other central potentials and plasma systems is highly required. Especially, it is desirable to justify the existence of these degeneracies on other experimental plasmas. Investigation of Hellmann-Feynman theorem for confined plasmas is necessary. Further, investigation of photo-ionization cross-section, relative information, two-photon transition amplitude, in *confined* and *shell-confined* plasmas would provide vital insight. Moreover, present study can be extended to many-electron atomic plasmas.

## VI. ACKNOWLEDGEMENT

NM thanks CSIR, New Delhi, India, for a Senior Research Associate-ship (Pool No. 9033A). The author acknowledges Prof. A. K. Roy for laboratory support and several valuable comments.

- 
- [1] A. Solyu. Phys. Plasmas, **19**, 072701 (2012).
  - [2] S. Paul and Y. K. Ho. Phys. Rev. A, **79**, 032714 (2009).
  - [3] E. Babaev, A. Sudbø, and N. W. Ashcroft. Nature, **431**, 666 (2004).
  - [4] D. J. Stevenson and N. W. Ashcroft. Phys. Rev. A, **9**, 782 (1974).

- [5] T. Guillot. *Phys. Today*, **57**, 63, (2004).
- [6] E. Gregoryanz, C. Ji, P. Dalladay-Simpson, B. Li, R. T. Howie, and H.-K. Mao. *Matter Radiat. Extremes*, **5**, 038101, (2020).
- [7] H. M. Van Horn. *Science*, **252**, 384 (1991).
- [8] M. S. Murillo. *Phys. Plasmas*, **11**, 2964 (2004).
- [9] M. Das. *Phys. Plasmas*, **21**, 012709 (2014).
- [10] N. Mukherjee, C. N. Patra, and A. K. Roy. *Phys. Rev. A*, **104**, 012803 (2021).
- [11] C. Martinez-Flores and R. Cabrera-Trujillo. *Matter Radiat. Extremes*, **3**, 227 (2018).
- [12] S. Paul and Y. K. Ho. *Phys. Plasmas*, **16**, 063302 (2009).
- [13] M. K. Bahar and A. Solyu. *Phys. Plasmas*, **092703**, 21 (2014).
- [14] M. K. Bahar, A. Soyulu, and A. Poszwa. *IEEE Trans. Plasma Sci.*, **44**, 2297 (2016).
- [15] H. E. Montgomery Jr., K. D. Sen, and J. Katriel. *Phys. Rev. A*, **97**, 022503 (2018).
- [16] S. Paul and Y. K. Ho. *Phys. Plasmas*, **15**, 073301 (2008).
- [17] Y.-D. Jung. *Phys. Plasmas*, **332**, 2 (1995).
- [18] Y.-D. Jung and J.-S. Yoon. *J. Phys. B*, **29**, 3549 (1996).
- [19] M. Y. Song and Y.-D. Jung. *Phys. Plasmas*, **36**, 2119 (2003).
- [20] F. A. Gutierrez and J. Diaz-Valdés. *J. Phys. B*, **27**, 593 (1994).
- [21] J.-S. Yoon and Y.-D. Jung. *Phys. Plasmas*, **3**, 3291 (1996).
- [22] L. R. Zan, L. G. Ziao, J. Ma, and Y. K. Ho. *Phys. Plasmas*, **24**, 122101 (2017).
- [23] C. Stubbins. *Phys. Rev. A*, **48**, 220 (1993).
- [24] Y.-D. Jung. *Phys. Plasmas*, **4**, 21 (1997).
- [25] Y. Y. Qi, J. G. Wang, and R. K. Janev. *Phys. Rev. A*, **80**, 063404 (2009).
- [26] L. Liu and J. G. Wang. *J. Phys. B*, **41**, 155701 (2008).
- [27] L. Liu, J. G. Wang, and R. K. Janev. *Phys. Rev. A*, **77**, 042712 (2008).
- [28] A. Poszwa and M. K. Bahar. *Phys. Plasmas*, **22**, 012104 (2015).
- [29] B. Saha, P. K. Mukherjee, and G. H. F. Diercksen. *Astron. Astrophys.*, **396**, 337 (2002).
- [30] Y. Y. Qi, J. G. Wang, and R. K. Janev. *Phys. Rev. A*, **78**, 062511 (2008).
- [31] Y. Y. Qi, Y. Wu, J. G. Wang, and Y. Z. Qu. *Phys. Plasmas*, **16**, 023502 (2009).
- [32] Y. Y. Qi, J. G. Wang, and R. K. Janev. *Phys. Rev. A*, **80**, 032502 (2009).
- [33] M. Bassi and K. L. Baluja. *Indian J. Phys.*, **86**, 961 (2012).
- [34] B. Saha and P. K. Mukherjee. *Phys. Lett. A*, **302**, 105 (2002).

- [35] L. Zhu, Yu. Ying He, L. G. Jiao, Y. C. Wang, and Y. K. Ho. *Phys. Plasmas*, **27**, 072101 (2020).
- [36] M. Das. *Phys. Plasmas*, **19**, 092707 (2012).
- [37] S. Kang, Y. C. Yang, J. He, F. Q. Xiong, and N. Xu. *Cent. Eur. J. Phys.*, **11**, 584 (2013).
- [38] J. K. Saha, T. K. Mukherjee, P. K. Mukherjee, and B. Fricke. *Eur. Phys. J. D*, **62**, 205 (2011).
- [39] C. Yadav, S. Lumb, and V. Prasad. *Eur. Phys. J. D*, **75**, 21 (2021).
- [40] P. K. Shukla and B. Eliasson. *Phys. Lett. A*, **372**, 2897 (2008).
- [41] L. G. Jiao, Y. Y. He, Y. Z. Zhang, and Y. K. Ho. *J. Phys. B*, (2021).
- [42] C. S. Lam and Y. P. Varshni. *Phys. Rev. A*, **6**, 1391 (1972).
- [43] C. S. Lai. *Phys. Rev. A*, **26**, 2245 (1982).
- [44] D. Singh and Y. P. Varshini. *Phys. Rev. A*, **28**, 2606 (1983).
- [45] R. Dutt, U. Mukherji, and Y. P. Varshini. *J. Phys. B*, **19**, 3411 (1986).
- [46] O. Bayrak and I. Boztosun. *Int. J. Quant. Chem.*, **107**, 1040 (2007).
- [47] C. Y. Lin and Y. K. Ho. *Eur. Phys. J. D*, **57**, 21 (2010).
- [48] S. Paul and Y. Ho. *Comput. Phys. Comm.*, **182**, 130 (2011).
- [49] I. Nasser, M. S. Abdelmonem, and A. Abdel-Hady. *Phys. Scr.*, **84**, 045001 (2011).
- [50] A. K. Roy. *Int. J. Quant. Chem.*, **113**, 1503 (2013).
- [51] H. F. Lai, Y. C. Lin, C. Y. Lin, and Y. K. Ho. *Chin. J. Phys.*, **51**, 73 (2013).
- [52] Y. Y. Qi, J. G. Wang, and R. K. Janev. *Phys. Plasmas*, **23**, 073302 (2016).
- [53] C. Y. Lin and Y. K. Ho. *Comp. Phys. Commun.*, **182**, 125 (2011).
- [54] C. G. Diaz, F. M. Fernández, and E. A. Castro. *J. Phys. A*, **24**, 2061 (1991).
- [55] S. Lumb, S. Lumb, and M. K. Bahar. *Phys. Rev. A*, **90**, 032505 (2014).
- [56] A. K. Roy. *Int. J. Quant. Chem.*, **116**, 953 (2016).
- [57] W. Grochala, R. Hoffmann, J. Feng, and N. W. Ashcroft. *Angew. Chem. Int. Ed.*, **46**, 3620 (2007).
- [58] A. K. Roy. *Int. J. Quant. Chem.*, **115**, 937 (2015).
- [59] R. T. Howie, C. L. Guillaume, T. Scheler, A. F. Goncharov, and E. Gregoryanz. *Phys. Rev. Lett.*, **108**, 125501 (2012).
- [60] R. T. Howie, P. Dalladay-Simpson, and E. Gregoryanz. *Nature Mater.*, **14**, 495 (2015).
- [61] R. P. Dias and I. F. Silvera. *Science*, **355**, 715 (2017).
- [62] V. L. Ginzburg. *Rev. Mod. Phys.*, **76**, 981 (2004).

- [63] J. M. McMahon, M. A. Morales, C. Pierleoni, and D. M. Ceperley. *Rev. Mod. Phys.*, **84**, 1607 (2012).
- [64] E. Wigner and H. B. Huntington. *J. Chem. Phys.*, **3**, 764 (1935).
- [65] M. D. Knudson, M. P. Desjarlais, A. Becker, R. W. Lemke, K. R. Cochrane, M. E. Savage, D. E. Bliss, T. R. Mattsson, and R. Redmer. *Science*, **348**, 1455 (2015).
- [66] S. T. Weir, A. C. Mitchell, and W. J. Nellis. *Phys. Rev. Lett.*, **76**, 1860 (1996).
- [67] N. W. Ashcroft. *Phys. Rev. Lett.*, **21**, 1748 (1968).
- [68] P. Dalladay-Simpson, R. Howie, and E. Gregoryanz. *Nature*, **529**, 63 (2016).
- [69] K. D. Sen, J. Garza, R. Vargas, and N. Aquino. *Phys. Lett. A*, **295**, 299 (2002).
- [70] K. F. Herzfeld. *Phys. Rev.*, **29**, 701 (1927).
- [71] N. Mukherjee and A. K. Roy. *Phys. Rev. A*, **104**, 042803 (2021).
- [72] A. L. Efros and D. J. Nesbitt. *Nature Nanotechnology*, **11**, 661 (2016).
- [73] Z. Fei, Z. Wang, D. Li, F. Xue, C. Cheng, Q. Liu, X. Chen, M. Cui, and X. Qiao. *Nanoscale*, **13**, 10765 (2021).
- [74] E. M. Nascimento, F. V. Prudente, M. N. Guimarães, and A. M. Maniero. *J. Phys. B*, **44**, 015003 (2011).
- [75] H. Peng, C. Rao, N. Zhang, X. Wang, W. Liu, W. Mao, L. Han, P. Zhang, and S. Dai. *Angew. Chem. Int. Ed.*, **57**, 8953 (2018).
- [76] C. Rao, C. Peng, H. Peng, L. Zhang, W. Liu, X. Wang, N. Zhang, and P. Wu. *ACS Appl. Mater. Interfaces*, **10**, 9220 (2018).
- [77] T. Raj kumar, G. Gnana kumar, and Arumugam Manthiram. *Adv. Energy Mater.*, **9**, 803238 (2019).
- [78] Y. Lai, W. Xia, J. Li, J. Pan, C. Jiang, Z. Cai, C. Wu, X. Huang, T. Wang, and J. He. *Electrochimica Acta*, **375**, 137966 (2021).
- [79] M. Fan, D. Liao, M. F. Aly Aboud, I. Shakir, and Y. Xu. *Angew. Chem. Int. Ed.*, **59**, 8247 (2020).
- [80] A.-C. Shi and B. Li. *Soft Matter*, **9**, 1398 (2013).
- [81] M. R. Khadilkar and A. Nikoubashman. *Soft Matter*, **14**, 6903 (2018).
- [82] G. Gnana kumar, S.-H. Chung, T. Raj kumar, and Arumugam Manthiram. *ACS Appl. Mater. Interfaces*, **10**, 20627 (2018).
- [83] W. Shuang, H. Huang, L. Kong, M. Zhong, A. Li, D. Wang, Y. Xu, and X.-H. Bu. *Nano*

- Energy, **62**, 154 (2019).
- [84] J. Wang, L. Zhu, F. Li, T. Yao, T. Liu, Y. Cheng, Z. Yin, and H. Wang. *Small*, **16**, 2002487 (2020).
- [85] D. E. Hastings and H. D. H. Stöver. *ACS Appl. Polym. Mater.*, **1**, 2055 (2019).
- [86] L. Qin, C. Li, X. Li, X. Zhang, C. Shen, Q. Meng, L. Shen, Y. Lu, and G. Zhang. *J. Mater. Chem. A*, **8**, 1929 (2020).
- [87] M. Zhang, C. Xiao, X. Yan, S. Chen, C. Wang, R. Luo, J. Qi, X. Sun, L. Wang, and J. Li. *Environ. Sci. Technol.*, **54**, 10289 (2020).
- [88] K. D. Sen. *J. Chem. Phys.*, **122**, 194324 (2005).
- [89] A. K. Roy. *Mod. Phys. Lett. A*, **29**, 1450104 (2014).
- [90] A. K. Roy. *J. Math. Chem.*, **52**, 1405 (2014).
- [91] A. K. Roy. *Mod. Phys. Lett. A*, **29**, 1450042 (2014).
- [92] N. Mukherjee and A. K. Roy. *Int. J. Quant. Chem.*, **118**, e25596 (2018).
- [93] N. Mukherjee and A. K. Roy. *Phys. Rev. A*, **99**, 022123 (2019).
- [94] N. Mukherjee and A. K. Roy. *J. Phys. B*, **53**, 235002 (2020).
- [95] S. Majumdar and A. K. Roy. *Quant. Rep.*, **2**, 189 (2020).
- [96] S. Majumdar and A. K. Roy. *Int. J. Quant. Chem.*, **121**, e26630 (2021).
- [97] A. Dalgarno. *Adv. Phys.*, **11**, 281 (1962).
- [98] R. C. Hilborn. *Am. J. Phys.*, **50**, 982 (1982).